NTNU – Trondheim
Norwegian University of
Science and Technology

Simulation and Evaluation of Slurry Erosion

Erik Grimm Strømme

Master of Science in Mechanical Engineering
Submission date: June 2015
Supervisor: Reidar Kristoffersen, EPT
Co-supervisor: Stein Tore Johansen, EPT
                          Jone Rivrud Rygg, Aker Solutions

Norwegian University of Science and Technology
Department of Energy and Process Engineering

NTNU

Norwegian University
of Science and Technology

Department of Energy
and Process Engineering

MASTER THESIS

for

Student Erik Grimm Strømme

Spring 2015

Simulation and Evaluation of Slurry Erosion

Simulering og evaluering av slurry erosjon

Background and objective

The purpose of the thesis is to assess computational methods for evaluating slurry erosion rates. A theory study should form the basis for proposing a method to evaluate this. That method should be validated against published literature, and if possible used to evaluate the erosion rate in an Aker-specific geometry exposed to slurry erosion.

The following tasks are to be considered:

- Study of relevant theory on slurry erosion and computational methods for evaluating this shall be studied and presented.
- An approach for numerical analysis of slurry erosion using Computational Fluid Dynamics (CFD) should be proposed. Relevant theory should be captured and the methodology should be compared to common practices assuming impact based erosion.
- Computational models to evaluate slurry erosion should be tested and validated against reference experimental data. Comparison to impact based particle erosion should be performed on the same cases.
- If possible, one computational model should be used to evaluate the erosion rate in an Aker-specific geometry

-- " --

Within 14 days of receiving the written text on the master thesis, the candidate shall submit a research plan for his project to the department.

When the thesis is evaluated, emphasis is put on processing of the results, and that they are presented in tabular and/or graphic form in a clear manner, and that they are analyzed carefully.

The thesis should be formulated as a research report with summary both in English and Norwegian, conclusion, literature references, table of contents etc. During the preparation of the text, the candidate should make an effort to produce a well-structured and easily readable report. In order to ease the evaluation of the thesis, it is important that the cross-references are correct. In the making of the report, strong emphasis should be placed on both a thorough discussion of the results and an orderly presentation.

The candidate is requested to initiate and keep close contact with his/her academic supervisor(s) throughout the working period. The candidate must follow the rules and regulations of NTNU as well as passive directions given by the Department of Energy and Process Engineering.

Risk assessment of the candidate's work shall be carried out according to the department's procedures. The risk assessment must be documented and included as part of the final report. Events related to the candidate's work adversely affecting the health, safety or security, must be documented and included as part of the final report. If the documentation on risk assessment represents a large number of pages, the full version is to be submitted electronically to the supervisor and an excerpt is included in the report.

Pursuant to "Regulations concerning the supplementary provisions to the technology study program/Master of Science" at NTNU §20, the Department reserves the permission to utilize all the results and data for teaching and research purposes as well as in future publications.

The final report is to be submitted digitally in DAIM. An executive summary of the thesis including title, student's name, supervisor's name, year, department name, and NTNU's logo and name, shall be submitted to the department as a separate pdf file. Based on an agreement with the supervisor, the final report and other material and documents may be given to the supervisor in digital format.

☐ Work to be done in lab (Water power lab, Fluids engineering lab, Thermal engineering lab)
☐ Field work

Department of Energy and Process Engineering, 14. January 2015
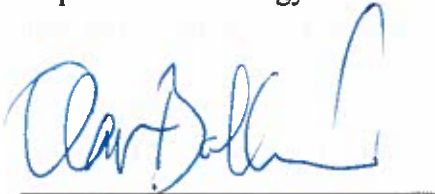
Olav Bolland
Department Head
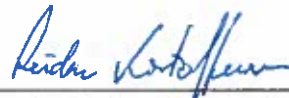
Reidar Kristoffersen
Academic Supervisor

Industrial Advisor: Robert Johansson, Aker Solutions
                       Jone Rivrud Rygg, Aker Solutions

Preface

This Master's thesis was written at the Department of Energy and Process Engineering at the Norwegian University of Science and Technology during the spring of 2015. The object of this thesis was developed in cooperation with the Subsea department at Aker Solutions.

First, I want to thank my academic supervisor, Reidar Kristoffersen for guidance and support during this semester. Also, big thank you to my two industrial advisors at Aker Solutions, Jone Rivrud Rygg and Guruprasad Kulkarni for your help, advice and important discussions during our weekly telephone-meetings. A thank you must also be given to Robert Johansson for providing me useful IT equipment and licenses, and to make this cooperation possible in the first place.

My sincere thank you goes to my fellow students at the Waterpower Laboratory for all the good discussions and the great work environment.

Last but not least, a special thank you to Benedicte, for motivating me every day along the way, also outside the grey walls. Your support has been invaluable.

Have fun!

Erik Grimm Strømme
Trondheim, June 2015

Abstract

Erosion from sand particles is a large problem in piping systems, especially in the oil and gas industries. Different types of erosion occur depending on the concentration of particles present in the fluid. Computational Fluid Dynamics (CFD) is a promising tool for erosion prediction, with different models available for erosion calculations. The most commonly studied erosion models are the Lagrangian impact based. These are simplified models, and they put a limit to model flows where particle concentrations increases.

The aim for this Master's thesis has been to investigate and assess available models in ANSYS Fluent for evaluating slurry erosion rates.

First, a literature study was carried out in order to understand how slurry flows behave under different flow conditions, how erosion from different sand particle concentrations are modeled and which models that are available ANSYS Fluent for these calculations. An important part of the study was to find available experimental results regarding erosion rates in literature, which could be replicated into CFD as validation of the erosion models.

The Lagrangian Discrete Phase Model (DPM) approach was used to validate the DNV erosion model against an experimental case with low particle concentration. A Slurry flow case simulation with the Eulerian model with a Dense Discrete Phase Model (DDPM) was set up on the same case in order to see if the model could capture the abrasive wear from the particles. All results from the DPM and DDPM simulations were written to file, plotted and compared with experimental results. Attempts were made in order to include the Discrete Element Method (DEM) collision model into the erosion simulations.

It was found that the DNV impact based erosion model shows good agreement with the experimental result by capturing the location and magnitudes of erosion rate. When including the Eulerian DDPM on the same geometry, results did not change much on the low particle concentration case. Thus, abrasive wear became more dominant as the particle concentration increased which is because of the increase of the wall shear stress from the slurry flow.

Since no suitable cases were found in literature regarding slurry erosion rates, an experimental case with higher particle concentrations should be performed so the models for slurry erosion can be validated.

Sammendrag

Erosjon fra sandpartikler er et stort problem når det kommer til rørsystemer, spesielt ved produksjon av olje og gass. Ulike typer av erosjon kan forkommer avhengig av konsentrasjonen partikler som er til stede i fluidet. Computational Fluid Dynamikk (CFD) er et nyttig verktøy for å beregne erosjon, med ulike erosjon modeller tilgjengelig for å utføre beregninger. Den mest brukte erosjonsmodellen er en Lagrange modell som baserer seg på enkelt partikler som treffer en overflate. Dette er forenklede modeller og egner seg ikke til modellering av løsninger med høyere partikkel konsentrasjoner.

Målet med denne masteroppgaven har vært å undersøke og vurdere tilgjengelige modeller i ANSYS Fluent for å evaluere erosjonsrater fra slurrier.

Først ble et litteraturstudie gjennomført for å forstå hvordan slurry-strømning oppfører seg under forskjellige strømningsforhold, hvordan erosjon fra ulike sandkonsentrasjoner kan modelleres og hvilke modeller som er tilgjengelig i ANSYS Fluent for denne type beregninger. En viktig del av studiet var å finne tilgjengelige eksperimentelle resultater vedrørende erosjonsrater, kopiere forsøket inn i CFD og bruke den for validering av erosjons-modellene.

For å validere DNVs erosjonsmodell mot eksperiment ble det benyttet en Lagrange Discrete Phase Model (DPM) tilnærming da partikkelkonsentrasjonen var lav. Det ble også gjort simuleringer på samme geometri for et tilfellet med høyere konsentrasjon av partikler. Her ble en Eulerian modell benyttet med en inkludert Dense Discrete Phase Model (DDPM) for å undersøke om modellen plukket opp slitasje fra partiklene som skled langs veggen. Resultatene fra DPM og DDPM ble skrevet til fil, plottet og sammenlignet med eksperiment-resultatene. Det ble i tillegg gjort forsøk på å inkludere kollisjonsmodellen Discrete Element Method (DEM) i simuleringene.

Erosjonsmodellen til DNV viste seg å gi gode resultater sammenlignet med eksperimentet, og fanget opp erosjonsratens størrelsesorden samt lokasjon. Simuleringer med Eulerian DDPM på den samme geometrien endret ikke resultatene stort for tilfellet med lav partikkelkonsentrasjon. Slitasjen fra partiklene derimot ble mer synlig og dominerende ettersom partikkel-konsentrasjonen økte, som var forventet på grunn av økningen av skjærspenningene på veggen fra slurrien. Siden ingen egnede eksperiment ble funnet i litteraturen for å validere slurry erosjonsmodellen, bør det utføres et eksperiment med høyere partikkelkonsentrasjoner.

Contents

List of Figures

List of Tables

Nomenclature

C_v solid concentration by volume

C_w solid concentration by mass

ρ_m mixture density

ρ_s solid density

ρ_l liquid density

ΔP pressure drop

f_{sl} friction factor

$\dot{E}$ erosion Rate

$\dot{m}_P$ particle mass flow rate

K material constant

n material constant

V_P^n particle impact velocity

A_t target area exposed to erosion

ρ_t target density

C_{unit} conversion factor

$F(\alpha)$ ductility of target material

α impact angle

A_i constants

S_{ij} rate of stress tensor

δ_{ij} kronecker delta-tensor

F_{all} sum of forces acting on particles

$\varnothing$ generic transported value

F_D drag force

u_p particle velocity

u fluid velocity

η_s Coulumbic friction

α_s particle volume fraction

α_{sp} packing volume fraction

τ linearization coefficient

C_D drag force coefficient

Re Reynolds number

τ_{ij} stress tensor

y^+ dimensionless distance

u^+ near wall velocity

U_t tangential velocity

τ_ω wall shear stress

u_τ skin friction velocity

κ von Karman constant

B log layer constant

k_e turbulent kinetic energy

ω turbulent frequency

μ_t turbulent viscosity

Abbreviations

ANSYS   Analysis Systems

CFD   Computational Fluid Dynamics

DDPM   Dense Discrete Phase Model

DEM   Dense Element Method

DNV   Det Norske Veritas

DPM   Discrete Phase Model

RANS   Reynolds Averaging Navier-Stokes

SIMPLE   Semi-Implicit Method for Pressure Linked Equations

SST   Shear Stress transport

1. Introduction

Erosive wear of both production and injection pipes is a big problem in the petroleum industry, where the consequences can be crucial. A mixture of water, oil, gas and sand particles are transported through miles of pipeline, and due to variation of velocities and the fluid properties, material loss in different equipment is considered a risk. It is therefore desirable to be able to accurately predict the rate of erosion.

The most commonly studied erosion mechanism is particle impact based erosion, calculating material removal based on particle impact velocity and angle. Particle impact based erosion is a risk mainly in gas and water flows where particles are suspended in the fluid. Another erosion mechanism often seen in the oil and gas industry is the slurry erosion. This happens due to the wall shear stress of the slurry along the pipe. These slurries are fluids with a large amount of solids, and this type of erosion can be seen even at low fluid velocities as the particles are sliding along a surface. Operations such as for instance drilling, cementing involve the use of slurries transported through the system.

Computational Fluid Dynamics (CFD) is a useful tool for predicting erosion. Even though the CFD modeling of erosion have been done for years, there is still a need of deeper knowledge about the models and methods available in the programs. Particle impact based erosion models available in CFD are only valid for specific low particle loading cases since the model neglects the occupied volume by the particles. This is an Eulerian-Lagrangian modeling of dispersed particles, and puts a limit to model flows as particle loadings increase. At higher particle loading, which is arguably the general case for slurry transport, particle to particle interaction comes into play. In general, slurry erosion is much more complex than particle impact erosion, making it difficult to predict. The simulation of these flows should be treated as fully coupled with an Eulerian-Eulerian approach. A method for prediction of slurry erosion is the topic of this thesis, where both Lagrangian and Eulerian models available in CFD should be tested for flow with higher particle loading.

In this thesis, an attempt has been made to develop a method using ANSYS Fluent as CFD software to model erosion from a slurry flow with a particle concentration higher than accepted for the Lagrangian impact based models. The DNV, Lagrangian approached impact based erosion model was first validated against experimental erosion results on a Bean Choke, reported by Huser & Kvernvold (1998). With this model validated, an Eulerian model with the

Dense Discrete Phase Model (DDPM) as an Eulerian parameter was set up and simulated in Fluent.

An experimental test case with higher particle concentration, reported by Loewen (2013), was supposed to be used as validation case for the Eulerian DDPM model. It appeared that the wall material used in the test-section was a polymer and not a metal. This became a problem in the simulations since the available models in Fluent require material constants, which are only available for some metals. Because of this, the experimental results were not suitable for the erosion model validation. Instead, the experimental results regarding the flow field and particle distribution were used to set up the Eulerian DDPM simulations. Simulations with this setup were then performed on the same Bean Choke geometry from Huser & Kvernvold (1998) in order to see the effect on erosion when the particle concentration was increased.

By using the different, available, erosion models, and the combination of the validated particle impact wear model and the abrasive wear model from ANSYS, erosion rate results from a slurry flow were captured and reported. This thesis report should give a good explanation of how these results are obtained, through both relevant theory and the presentation of how the simulations have been performed.

2. Theory

This chapter is covering the relevant theory, and is divided into three sections. The first section describes the slurry flow and its physical properties. The second presents the most common erosion processes present in a pipeflow of a continuous phase and a solid phase. Both particle impact and sliding abrasion are described. In the third section, the theory behind the CFD simulations are described, and how ANSYS Fluent is solving the governing equations for these simulations.

2.1 Slurry flow

Slurries are a solid-liquid mixture with a large amount of solids. A slurry can sometimes be classified as a high viscous fluid. Since the particle concentration is high, it is important to understand the physical principles for this type of flow and also to classify the slurries. With the high particle concentration, the erosion phenomena will occur. Slurry erosion is an erosion mechanism that occur due to the wall shear of the slurry flow through a pipe combined with random particle impacts.

2.1.1   Physical properties and classification of a slurry

It is important to classify a slurry in order to provide a basis for describing the physical appearance and the flow behavior of the two-phase solid-liquid mixture, i.e. rheology. Rheology is the study of the flow of matter, and applies to substances with complex structures such as slurries. The rheology is a dynamic property of the microstructure of the slurry and is affected by various attributes such as the shape, density, size and mass fraction of the suspended solid particles and the density and viscosity of the carrier fluid (Roitto, 2014, p. 6).

The classification of the slurry flow is also important when it comes to designing pipelines. The most commonly used attributes used to characterize a slurry are the basic physical properties of the constituents, in particular those of the solids (Brown & Heywood, 1991, p. 3):

- *Density* of the constituent phase,
- *Concentration* of solids,
- Characteristic *particle size* or more appropriately, *particle size distribution* and
- Characteristic *particle shape*.

Depending on the particle size, it is usual to classify the particles as coarse, medium and fine particles depending on their diameter. ISO 14688-1 (2002) lists the basic principles for the

classification of different soils most commonly used for engineering purpose, and the size-range for sand is shown in Table 2.1 (ISO 14688-1, 2002):

Size range, d [mm]	Description
$0.063 \leq d \leq 0.2$	Fine
$0.200 \leq d \leq 0.63$	Medium
$0.630 \leq d \leq 2.0$	Coarse

Table 2.1: Sand particle definition (ISO 14688-1, 2002).

The *Density* of the slurry is affected by the density of the carrier fluid, the density of the solid particles and the concentration of solid particles present. The solid concentration can be expressed by volume or weight fraction. The relationship between these two can be expressed as (Wasp, 1977, p. 46):

$$C_V = \frac{C_w \rho_m}{\rho_s} = \frac{100 \dfrac{C_w}{\rho_s}}{\dfrac{C_w}{\rho_s} + \dfrac{100 - C_w}{\rho_l}} \tag{2.1}$$

where

C_v = concentration by volume in percent

C_w = concentration of solids by weight in percent

ρ_m = density of mixture [kg/m^3]

ρ_s = density of solid [kg/m^3]

ρ_l = density of liquid [kg/m^3]

And from this relation, the density of slurry is defined as (Wasp, 1977, p. 45):

$$\rho_m = \frac{100}{\dfrac{C_w}{\rho_s} + \dfrac{100 - C_w}{\rho_l}} \tag{2.2}$$

Depending on the particle concentration, slurries can be classified as a *dilute* or a *dense* slurry. A *dilute slurry* flows have a low particle volume concentration (<5-10%), where erosion occur mainly due to particle impact on the walls. For the *dense slurries* flows, the particle volume concentration is higher and the particle-particle interaction becomes more important than for dilute slurries (Brown & Heywood, 1991, pp. 7-8).

2.1.2 Describing Slurry flows

To understand the erosion phenomena in a solid-liquid pipe flow, it is important to look at the flow regimes in the dense slurry transport. Information of velocity and particle concentrations profiles will give an indication of the solids distribution in the pipe cross-section.

Depending on the particle size and velocity, slurries are usually associated with settling tendencies. If the velocity though a pipe is low and the particle size is large, particles will tend to sink and settle at the bottom pipe wall. This is called a *Newtonian, settling slurry*. If the particle size is smaller, the slurry can be classified as *a non-settling slurry* and may exhibit a *non-Newtonian* behaviour. Particles then remain in suspension for a long time. For a slurry flow through a pipe, velocity must then increase as particle size increases in order to avoid the slurry to settle and keep particles suspended (Brown & Heywood, 1991, pp. 41-42). If particles settle at lower speed, they can block the pipe as a worst case scenario.

Since non-Newtonian flow is very complex and a complete study itself, the viscous effects are neglected in this thesis. That means that the slurry flows are at any time defined as a both *settling* and *Newtonian,* and the viscosity of the fluid remains constant and is independent of any external stresses, and the shear rate that is affects it. An example can be the forces acting on the fluid from the particles.

By the settling tendency under the influence of gravity, transport of slurry flow can be classified into four different flow regimes in a horizontal pipe. Concentration is usually higher in the bottom layer of the cross-section, and the extent of the solid concentration is dependent on the velocity and the turbulence. With high velocity and high turbulence levels, the suspension is almost *homogeneous* with very good dispersion of the solids. With low turbulence levels, the particles will settle towards the wall and be transported as a *sliding bed* under the influence of the pressure gradient in the fluid. If the turbulence levels are not high enough to maintain a homogeneous suspense but still sufficiently high to prevent any deposition of particles on the wall in the pipe, the flow regime is described as a *heterogeneous suspension*. As the velocity of the slurry reduces further, a distinct mode of transport known as *saltation regime* develops. In this regime, there is a visible layer of particles in the bottom wall in the pipe, and they are being

continuously picked up by turbulent eddies along the pipe (King, 2002, pp. 83-84). The four flow regimes for settling slurries in horizontal pipes are shown in Figure 2.1.

Sliding bed

Saltation

Heterogenous suspension

Homogeneous supension
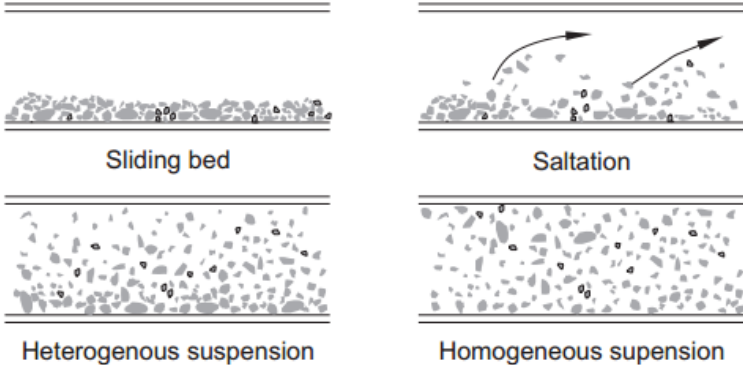
Figure 2.1: Four flow regimes for a settling, heterogeneous slurry in horizontal pipelines (King, 2002, p. 84).

The relationship between frictional pressure gradient and the slurry velocity varies from regime to regime and they can be approximately delimited in the particle size vs. slurry velocity as shown in Figure 2.2 (King, 2002, p. 84).

Sliding bed

Saltation

Heterogeneous suspension

Homogeneous suspension

Particle size

Slurry velocity
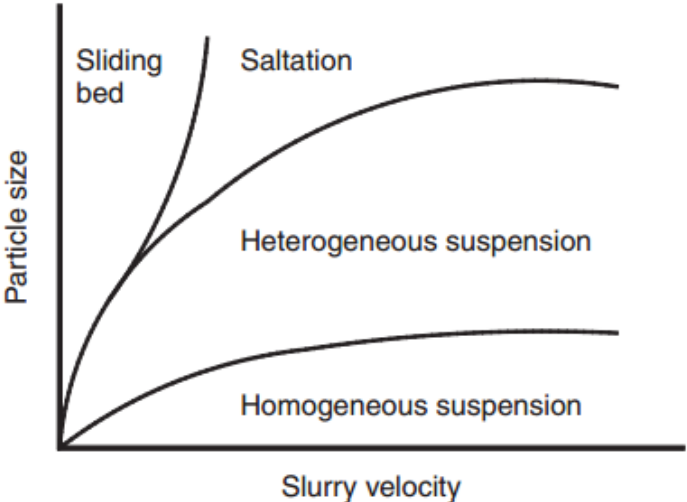
Figure 2.2: Schematic representation of the flow regimes for settling slurries in horizontal pipelines (King, 2002, p. 84).

2.1.3 Pressure gradient in slurry flows

With flow taking form of the four different regimes from a sliding bed of mud to a homogenous suspension, a number of different factors will interact in a horizontal pipe. With transportation of a settling, heterogeneous slurry, the influence of gravity will develop significant gradients in the solid concentration. The solids will generate additional momentum transfer and need to be

considered when developing models for momentum transfer between the slurry and the pipe wall. Particles moving faster than the fluid will transfer some of its momentum to the fluid, and faster moving fluid will transfer momentum to the particles. This interaction with solid particles and liquid in a two-phase flow, will also affect the momentum transfer from the two-phase to the wall. Particles will dissipate some of their kinetic energy by hitting the wall. This will increase the shear stresses from the fluid-particle and the wall, i.e. higher friction drag force through the pipe (King, 2002, pp. 81-82). The additional path through which momentum can be transferred from the fluid to the solid wall during a settling slurry through a pipe can be illustrated as done in Figure 2.3 (King, 2002, p. 82).
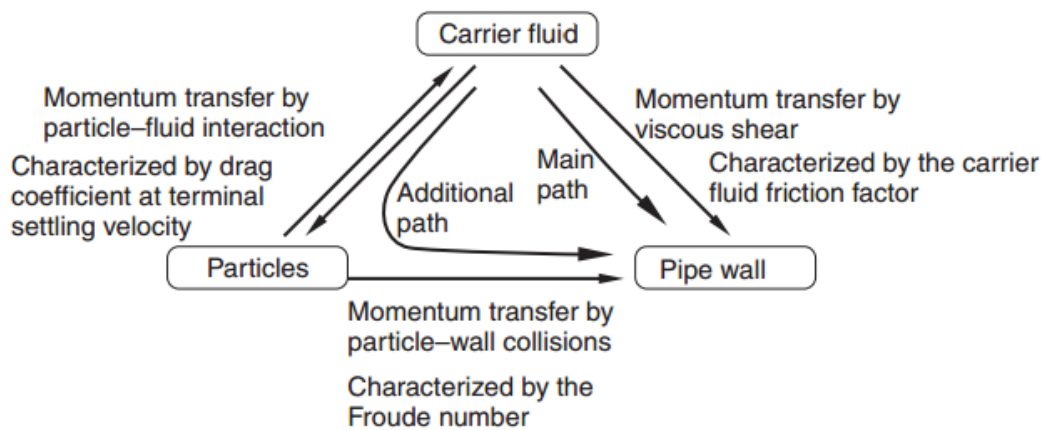
Figure 2.3: Momentum transfer between the fluid and the wall during slurry flows through a pipe (King, 2002, p. 82).

This additional momentum transfer through the pipe will affect the pressure drop because of friction from the particles. Compared to the pressure drop through the pipe with only a single fluid present, the solid particles momentum transfer will increase the pressure drop. This is expressed in equation 2.3 (King, 2002, p. 82).

$$\Delta P_{f,sl} = \Delta P_{fw} + \Delta P_{additional} \tag{2.3}$$

Where $\Delta P_{f,sl}$ is the pressure drop due to friction from the slurry transport, ΔP_{fw} is the pressure gradient if only the fluid were present flowing at the same velocity as the slurry. This pressure gradient can also be calculated from the relationship between the wall shear stress and pressure gradient, and *vice versa* (King, 2002, p. 82).

$$\Delta P_{f,sl} = f_{sl}\rho_w \overline{V}^2 \frac{L}{2D} \tag{2.4}$$

where ρ_w is the density of water and not the slurry density.

By calculating the pressure drop, and then the friction factor, it is possible to use the Moody diagram to find the friction coefficient ε in the pipe with particles in the domain.

A typical pressure drop – velocity relation of a heterogeneous slurry flow through a pipe is given in Figure 2.4. The pressure drop with only water present in the pipe is also shown as a comparison (Mali et. al, 2014, p. 2).
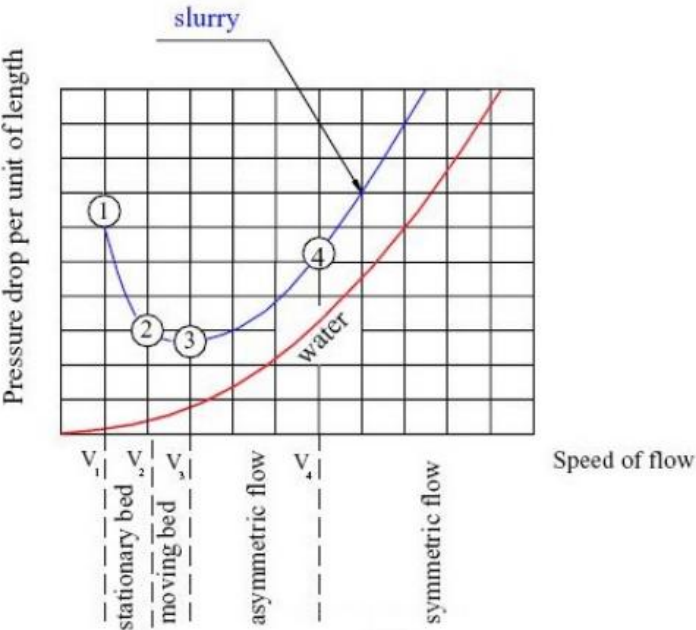
Figure 2.4: Pressure drop – velocity relation of heterogeneous slurry flow through a pipe (Mali et. al, 2014, p. 2).

At higher velocities *(point 4)* the curve tend to be parallel to the simple fluid response through the pipe. At higher velocities than 4, slurry flow becomes homogenous and the concentration gradient becomes less dominant. As the velocity decreases, the solids are still suspended, but the distribution becomes heterogeneous. When the velocity reach point 3, the solids start to form a sliding bed i.e. saltation regime. At this point, the slurry reach the critical velocity, where the pressure drop is at its minimum. With an even further speed reduction of the flow *(point 2)*, more of the solids are transported as a bed load through the pipe. This tendency of particles settling as a stationary bed increases until point 1, where the solids stop moving (Mali et. al, 2014, pp. 1-2).

The critical velocity *(point 3)* is the most useful since at this point the head loss is at its minimum, and is defined as when particles are no longer transported through the pipe in suspension or whether or not the bed is moving or stationary (Wasp, 1977).

8

2.2 Erosion

Erosive wear, commonly known as *erosion* is defined as material loss resulting from impact of solid particles on the material surface (DNV, 2007, p. 10). In complex piping systems, with sand particles present in the fluid, particles sliding, rolling, colliding or hitting the material surface will result in material deformation, cutting, fatigue cracking or a combination of these.

With different influencing factors on erosion from sand particles, different types of wear mechanisms can occur. Before going deeper into the types of wear relevant for this thesis, a list of some relevant wear mechanisms from particle impacts are listed in Table 2.2 (Meng & Lundema, 1995, pp. 449-450):

Mechanism of erosion	Definition	Illustration
Abrasive erosion	Particles strike the wall at low impact angles and material is removed by cutting. The particles act like a bed that is sliding over the surface.	
Fatigue wear	Particles strike the surface at low speed, but a with a large impact angle. The surface material cannot be plastically deformed, but it becomes weak due to fatigue action. After repeated hits, cracks will occur in the material and particles will be detached from the surface after multiple hits	
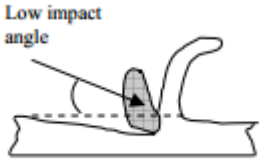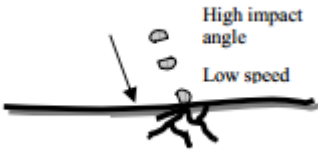
Brittle fracture	Erosion by brittle fracture when particles hit the wall with medium velocity and high impact angle. This is likely to happen when the particles have sharp edges.	
Saltation wear	Transport of a sediment where particles are moved forward along the pipe in series, bouncing along the wall.	
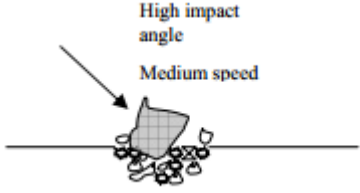
Table 2.2: Different types of wear from sand particles.

From the different definitions above, it is clear that the extent of the removed material is dependent on various parameters such as particle and material properties, flow conditions and the particle volume fraction present in the fluid flow. These are listed in Table 2.3 (Eltvik, 2013, p. 9):

Flow conditions	Relative velocities between interacting surfaces- Impact velocity, impact angle, particle mass flow rate, turbulence-, centrifugal-, cavitation forces, viscosity
Particle properties	Particle size, density, shape and concentration
Material properties	Material hardness, ductility, coating, strength

Table 2.3: Parameters affecting erosion (Eltvik, 2013, p. 9).

During transport of slurries through a pipe at a typical bulk velocity, the particles settle at the lower pipe wall due to gravitational forces. This creates a dense, sliding bed of particles that moves slower than the fluid along the pipe. This action of the solid bed inflicts the erosive damage on the pipe walls. This is the wear mechanism better known as *abrasive wear* and is one of the main wear mechanisms in *slurry erosion*. The remaining particles above the bed is assumed to be suspended by turbulence effects and particle lift forces. These effects cause particles to impinge against the pipe walls, and this erosion effect is called *impact based erosion*. These are the two dominant erosion models in slurry transport, and are described in the following chapters.

2.2.1 Particle impact erosion

Solid particle erosion is the loss of material that results from repeated impact on a surface of small, solid particles. This type of erosion can be expected in any gas or liquid flow with hard particles present. The particles are affected by the fluid which carries them along the flow (Kosel, 1992, p. 199).

The first models developed for predicting erosion are based on the movement of a single particle. Since then, different models have been developed in order to calculate erosion from solid particles, and what they have in common are that they all requires a lot of input about the flow conditions and the particles parameters. If these parameters are known, the erosion rate, $\dot{E}$ can be calculated from the general relation in the Recommended Practice written by Det Norske Veritas, DNV (DNV, 2007, p. 14):

$$\dot{E} = \frac{\dot{m}_P \cdot K \cdot V_P^n \cdot F(\alpha)}{\rho_t \cdot A_t} C_{unit} = \frac{\dot{E}_m}{\rho_t \cdot A_t} 10^3 \left[\frac{mm}{yr} \right] , \quad C_{unit} = 3.15E10 \tag{2.5}$$

where

$\dot{m}_P$, is the particles mass flow rate.

K and n, is the material constants, which are determined by experimental investigations given in Table 2.4 (DNV, 2007, p. 11).

Material	K [(m/s)$^{-n}$]	n [-]	P [kg/m^3]
Steel	2.0×10^{-9}	2.6	7800

Table 2.4: Material constants for steel (DNV, 2007, p. 11)

V_P^n, is the impact velocity of particle and n is a material constant.

A_t, is the area exposed to erosion, target area.

ρ_t, is the targets density.

C_{unit}, is a conversion factor from [m/s] to [mm/year].

The function $F(\alpha)$ characterises the ductility of the target material, given by the relation;

$$F(\alpha) = \sum (-1)^{(i+1)} A_i \left(\frac{\alpha \cdot \pi}{180} \right)^i \tag{2.6}$$

where the A_i's are given in Table 2.5 (DNV, 2007, p. 10):

A_1	A_2	A_3	A_4	A_5	A_6	A_7	A_8
9.370	42.295	110.864	175.804	170.137	98.398	31.211	4.170

Table 2.5: Constants to be used in equation 2.6 (DNV, 2007, p.10).

In equation 2.6, α is the impact angle, which is defined as the angle between the particle and the wall. Figure 2.5 show the impact angle with a particle approaching the wall with a velocity, u (Huser & Kvernvold, 1998, p.4):
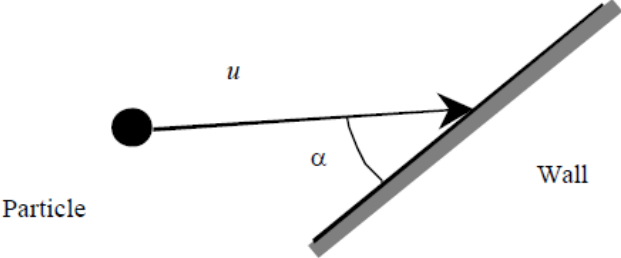
Figure 2.5: Impact angle definition (Huser & Kvernvold, 1998, p.4).

Ductile materials attain maximum erosion attacks for impact angles in the range of 15°-30° while brittle materials at a normal impact angle. For this thesis, the steel grades are regarded as ductile material. The relationship between function F(α) an the impact angle is shown in Figure 2.6 (DNV, 2007, p. 12).
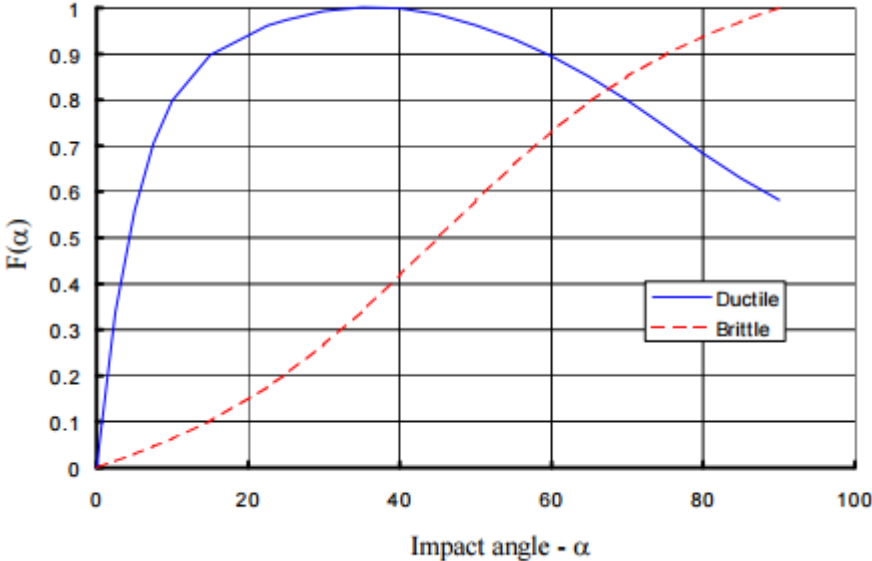
Figure 2.6: Function F(α) for typical 'ductile' and brittle materials (DNV, 2007)

12

In the DNV erosion model, the blue curve for ductile material is used as the boundary condition on the wall for the particle impact function. More details on this is described later in this thesis.

2.2.2 Slurry erosion

Slurry erosion is defined as the type of wear that occur when a material is exposed to a slurry flow of higher particle loading. Shook & Roco (1991) have defined the erosion in dense slurry flow as having three components including *direct impact of particles*; *random impingement* of particles in turbulent motion and the friction of a sliding bed of particles pressing onto the wall, known as *abrasive wear*.

The slurry erosion phenomena is complex due to the number of important independent variables present that influence these three components. In Table 2.6, some of the main variables are listed (Wood et. al, 2001, p. 774):

Slurry variables

Liquid	Viscosity, density, surface activity, lubricity, corrosivity, temperature
Particles	Brittleness, size, density, relative velocity, shape, relative hardness, concentration, particle-particle interactions
Flow field	Angle of impingement, particle impact efficiency, boundary layer, wall shear stress, particle rebound, degradation, particle drop-out, turbulence intensity

Component variables

Bulk properties	Ductility or brittleness, hardness, melting point, microstructure, shape and roughness
Surface properties	Work hardening, corrosion layers, surface treatments, coating type, coating bond, microstructure

Service variables

	Contacting materials, pressure, velocity, temperature, surface finish, lubrication, corrosion, hydraulic design, intermittent slurry flows.

Table 2.6: Important independent variables present that influence slurry erosion (Wood et. al, 2001, p. 774).

In a slurry pipeline, the hydraulic gradients, i.e. head losses, are a key parameter. In literature, the main component of head loss that is documented, which is contributing to wear from a slurry, is the velocity independent Coulombic friction. The *Coulombic friction* is the relation between particle stresses in different direction. For example by saying that τ_{yy} is fixed by gravity, and if motion occurs in x-direction the stresses are related by a coefficient of Coulombic friction, η_s (Gillies, 1993, p. 15):

$$\tau_{yx} \sim \eta_s \tau_{yy} \tag{2.7}$$

This coefficient depends on the nature of the two surfaces and is caused by sliding motions of the particles along the pipe wall. Lubrication effects reduce the coefficient of friction for particles, which is moving parallel to the wall, if a liquid layer is separating them. Therefore, this friction coefficient can be neglected further away from the wall, since the particles is fully suspended in this area.

Based on results published in literature, the Coulombic friction is high at low velocities where particles experience minimal lifting force. At higher velocities, the Coulombic friction diminishes as the particle-bed cross-section diminishes (Loewen, 2013, p. 20). The minimum friction occur at the critical velocity as presented in chapter 2.1.3.

Slurry erosion is dependent on various parameters as mentioned above, but more important is how the flow-field looks like and how high the particle loading is. As described in chapter 2.1.2, the classification of the slurry is dependent on the concentration of the solid and fluid properties. The amount of abrasive wear is dependent on the particle concentration and again by the bulk velocity through the pipe. By increasing the velocity, avoiding particles to settle, the erosion damage due to particle impact will increase as the flow is more heterogeneous and particles are suspended in the fluid. This will also reduce the abrasive wear along.

2.2.3 Experimental methodologies for predicting erosion

Erosion studies have been performed for many years, and many different methods have been used to get experimental results when it comes to wear of materials from sand particles. Experiments have focused on sand concentration profiles, velocity profiles and frictional pressure gradients. These results have been important in order to understand the flow field with different particle loading. When it comes to experimental results regarding erosion rate, or just material removal, not much have been reported. One of the benefits with a laboratory test is that it is possible to have control over a wide range of parameters, for example sand

concentration, which is a varying factor in the actual cases in nature. These are complex experiments, and as discussed earlier; many factors and parameters must be taken into account to keep control of the experiment.

In this thesis's literature study, a lot of time have been spent in order to find reliable experiments to replicate and model into CFD, and to compare the numerical results with the experiment. It should be possible to see how good the CFD predicts erosion, both the impact based and the slurry erosion. The focus have been to find data from tests performed in pipes so it is easier to relate the results to the actual case for oil-production. In general, the pipe loop tests are small scale versions of the real pipes. In order to have fully control of the flow, there is a flow controller in the loop. The loop usually includes more than one test section with different geometries; straight pipe, t-bends and 90° bends are some examples. In this chapter, the experiments that are used and replicated in this thesis are presented briefly.

An experiment reported by DNV is used as a test for the Lagrangian erosion models (Huser & Kvernvold, 1998, pp. 5-6). Carbon-dioxide gas at subsonic speed is sent through a B*ean Choke* as shown in Figure 2.7. The gas enters a large diameter pipe, goes through a contraction and exits through a smaller diameter outlet-pipe. It is clear that the velocity will increase as the area after the contraction is lower, and it is expected that the fluid especially in this area will affect particles. The following flow and particle parameters are applied to the experiment (Huser & Kvernvold, 1998, pp. 5-6):

- Inlet velocity: 11,4 [m/s]
- Inlet pressure: 14.1 [bar]
- Inlet temperature: 36 ºC
- Fluid Viscosity: 1.5×10^{-5} [kg/(ms)]
- Inlet diameter: 54 mm
- Outlet diameter: 20 mm
- Particle diameter: 0.25 mm
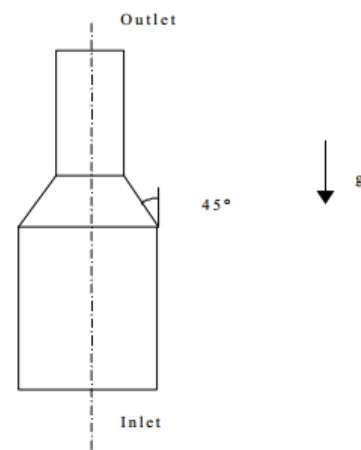
Figure 2.7: Bean Choke geometry (Huser & Kvernvold, 1998, p. 5).

The above experiment from DNV is suitable for testing impact based erosion models in CFD since the particle concentration is low. For denser slurries, there are limited with performed experiments available in literature regarding erosive wear and slurry erosion. The only reported case found in the literature study in this thesis is from the University of Alberta, US, where a large test-rig has been built and the master thesis student, Derek John Loewen, has reported his

experimental work regarding *Characterization of Wear in a Laboratory-Scale Slurry Pipeline* (2013). The experiment examines few selected parameters during the tests in order to understand the principal parameters and therefor these assumptions are made (Loewen, 2013, p. 51);

- Two-phase water-sand slurries are used in order to eliminate non-Newtonian effects, bitumen-related wall roughness and air bubbles affecting the flow.
- This allows focus to remain on mechanical wear, without being concerned with the compounding effects of corrosive and erosive-corrosive wear.
- Mass flow rate and bulk solids concentration is controlled within the process. Particle size and the sensitivity of the size is not included in the study, and an average size is kept constant.

The setup of the slurry loop design with all equipment is shown in Figure 2.8 (Loewen, 2013, p. 53).
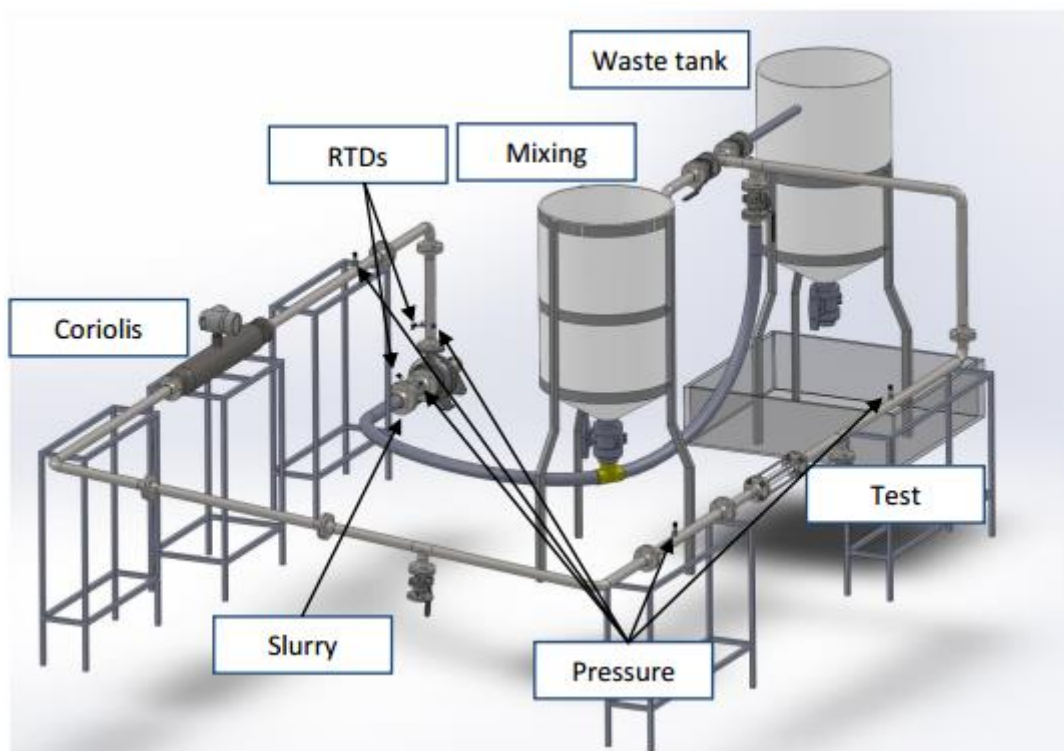
Figure 2.8: Slurry loop design with all equipment (Loewen, 2013, p.53).

The testing section is a removable tube-section that consists of a two slip-on steel flanges supported by four threaded rods. The test pieces may be fitted into the flanges and tightened in

place with nuts. The test material for the pipe-wall was first chosen to be PVC, but even after 65 hours of being subjected to slurry flow at high pump speed; the PVC did not show any visible scratches or signs of wear. Therefore, urethane was used as coating on the inner walls, with 2.7 mm thick layer (Loewen, 2013, pp. 64-65). Urethane is a polymer which have lower density than steel, and erosion from sand particles is easier to get visible.

The following flow and particle parameters were applied to the experiment:

- Outer pipe diameter: 57.15 mm
- Wall thickness: 2.7 mm
- Length of test section: 488.15 mm
- Particle concentrations: 6.4 and 13.5 [vol%]
- Average particle diameter: 1.5 mm
- Mass flow rate: ~5, ~6 and ~9 [kg/s]

Erosion rate results in [kg/hr/m] are given for different pump speeds i.e. mass flowrates.

2.3 Theoretical Background of Computational Fluid Dynamics

When modeling turbulent flow in pipes with sand present, the treatment near the wall is important to do correctly. This is because the turbulence can have a significant influence on erosion my particle impact. In Computational Fluid Dynamics (CFD), numerical methods and physical models are available for predicting the approximate mean motion and trajectories of particles suspended in turbulent flows (Dosanjh & Humphrey, 1985). This chapter provides a brief description of the CFD and the applications used in this thesis.

2.3.1 General

CFD is a set of numerical methods applied to obtain approximate solutions of problems of fluid dynamics and heat transfer (Zikanov, 2010, p. 1).

The equations governing the fluid flow have been known for a century. The equations are complex, but their solutions are very useful to understand fluid flows, regarding both the dynamics and heat transfer. Unfortunately, these equations cannot be solved in general. A numerical approach is used as a computational procedure to find an approximation to the solution. This approach outperforms the theoretical and the experimental approach in some very important aspects; universality, flexibility, accuracy and cost (Zikanov, 2010, pp. 2-3).

2.3.2 Governing Equations

Three governing equations describes the conservation laws of classic physics, namely:

- Conservation of mass
- Momentum equation
- Conservation of energy

In the process for the numerical approach solution, the fluid is regarded as a continuum; the substance fills the given space it occupies. The computational domain is divided into a certain number of small elements, where the elements are large enough compared with the sizes of the molecules to treat the fluid as a continuum. These elements are called *fluid elements* (Zikanov, 2010, pp. 11-12).

When the fluid moves through these elements, conservation laws must be satisfied and the equations can be presented on differential form;

The continuity equation requires conservation of mass:

$$\frac{\partial \rho}{\partial t} + \frac{\partial}{\partial x_i}\left(\rho u_i\right) = 0 \tag{2.8}$$

The Navier-Stokes equation is derived from the Newton's 2nd law:

$$\frac{\partial}{\partial t}\left(\rho u_i\right) + \frac{\partial}{\partial x_j}\left(\rho u_i u_j\right) = -\frac{\partial p}{\partial x_j} + \frac{\partial}{\partial x_j}(2\mu S_{ij} - \frac{2}{3}\mu\frac{\partial u_k}{\partial x_k}\delta_{ij}) + \rho f_i \tag{2.9}$$

where S_{ij} is the rate of strain tensor and δ_{ij} is the Kronecker delta-tensor

The energy equation is only necessary if the flow is compressible or with thermal conduction, which is not the case in this study.

ANSYS Fluent are using the finite volume technique by discretizing and solving the given equations above in each of the fluid elements. This is a control-volume-based technique consists of integrating the transport equation about each control volume. Starting with a transport equation on the integral form (ANSYS Fluent, 2013, 20.2.):

$$\int_V \frac{\partial(\rho\phi)}{\partial t}dV + \oint \rho\phi\vec{v}\cdot d\vec{A} = \oint\Gamma_\phi\nabla\phi\cdot d\vec{A} + \int_V S_\phi dV \tag{2.10}$$

The volume integrals is then discretized within the element and accumulated to the control volume to which the sector belongs. Surface integrals are discretized at the integration points located at the center of the each surface segment within the element and then distributed to the adjacent control volumes:

$$\frac{\partial(\rho\phi)}{\partial t}V + \sum_f^{N_{faces}}\left(\rho_f\phi_f\vec{v_S}\right)\cdot\vec{A}_f = \sum_f^{N_{faces}}\Gamma_\phi\nabla\phi_f\cdot A_f + S_\phi V \tag{2.11}$$

with subscript *f* as a value within the control volume (ANSYS Fluent, 2013, 20.2.). With just a few adjustments, equation (2.10) can be used for each of the control volumes in the given domain. This will result in a set of algebraic equations that can be solved using iterative methods, such as conjugate gradient, multigrid etc.

2.3.3   Equation of Motion for Particles

ANSYS Fluent calculates the trajectory of a discrete phase particle by integrating the force balance on the particle, which is done in a Lagrangian approach. This force balance equates the particle inertia with forces acting on the particles such as drag, pressure, buoyancy and added mas or virtual forces. This can be written as (ANSYS Fluent, 16.2.1.1.):

$$\frac{d\vec{u}_p}{dt} = F_D(\vec{u} - \vec{u}_p) + \frac{\vec{g}(\rho_p - \rho)}{\rho_p} + \vec{F} \qquad (2.12)$$

where,

$\vec{u}$ is the fluid phase velocity,

$\vec{u}_p$ is the particle velocity,

ρ is the fluid density,

ρ_p is the density of the particle.

$F_D(\vec{u} - \vec{u}_p)$ is the drag force per unit particle mass and

$$F_D = \frac{18\mu}{\rho_p d_p^2} \frac{C_D \, \mathrm{Re}}{24} \qquad (2.13)$$

where,

μ is the molecular viscosity of the fluid,

Re is the relative Reynolds number, which is defined as

$$\mathrm{Re} \equiv \frac{\rho d_p \left| \vec{u}_p - \vec{u} \right|}{\mu} \qquad (2.14)$$

and the drag coefficient for spherical particles is taken from Morsi and Alexander (1972) experiments, with constants a_1, a_2 and a_3 that apply over several ranges of Re (Morsi & Alecander, 1972, p. 195) :

$$C_D = a_1 + \frac{a_2}{\mathrm{Re}} + \frac{a_3}{\mathrm{Re}^2} \qquad (2.15)$$

$\vec{F}$ in equation (2.12) is an additional *acceleration* term. This includes additional forces that can be special under different circumstances, and is defined under the physical setup for particles. For this thesis, the following additional forces are important (ANSYS Fluent, 2013, 16.2.1.3.):

1. *Virtual mass force* is required to accelerate the fluid surrounding the particle. This term can be written as:

$$\vec{F} = C_{vm} \frac{\rho}{\rho_p} (\vec{u}_p \nabla \vec{u} - \frac{d\vec{u}_p}{dt}) \qquad (2.16)$$

where C_{vm} is the virtual mass factor with default value of 0.5.

2. *Pressure gradient force* comes as an additional force which is arising from the pressure gradient in the fluid:

$$\vec{F} = \frac{\rho}{\rho_p} \, \vec{u}_p \nabla \vec{u} \tag{2.17}$$

The two forces are important when the density ratio between particle and fluid is greater than 0.1. This means that for a sand-gas flow, where $\rho/\rho_p \ll 1$, it is not important (ANSYS Fluent, 2013, 16.2.1.3.).

2.3.4 Turbulent modeling

The flow becomes turbulent above a critical Reynolds number (White, 1999, pp. 325-330).

$$\text{Re}_{crit} \approx 2300 \quad , \quad \text{Re} = \frac{\rho U D}{\mu}$$

Today, the most common approach in industry to solve the turbulence is by using the Reynold Averaging Navier-Stokes (RANS) model. For the RANS model, the pressure and velocity is decomposed into mean and fluctuating components:

$$u_i = \bar{u}_i + u_i^{'} \tag{2.18}$$

$$p = \bar{p} + p' \tag{2.19}$$

Introducing these expressions into the N-S equation (2.9) and averaging:

$$\rho \frac{\partial \bar{u}_i}{\partial t} + \rho \frac{\partial}{\partial x_j} \left(\overline{u_i^{'} u_j^{'}} \right) = \rho g - \frac{\partial p}{\partial x_i} + \mu \nabla^2 \bar{u}_i \tag{2.20}$$

also continuity; $\dfrac{\partial \bar{u}_i}{\partial x_i} = 0$

Rewriting the equation to include the stress tensor, from the relation: $\tau_{ij} = \mu \dfrac{\partial u_i}{\partial x_j} - \rho \left(\overline{u_i' u_j'} \right)$

Equation (2.20) becomes:

$$\rho \frac{\partial \bar{u}_i}{\partial t} = \rho g - \frac{\partial p}{\partial x_i} + \nabla \cdot \tau_{ij} \tag{2.21}$$

21

Performing the time-averaging operation on the momentum equations, all the details of the state of the fluid contained in the rapid fluctuations is gone. The result yields six additional unknown functions, which is the Reynold stresses. The main task of turbulence modeling is to develop computational procedures of sufficient accuracy and generality for engineers to predict the Reynolds stresses and the scalar transport terms (Versteeg & Malalasekera, 1996, 5, pp. 75-78). Before introducing the turbulence models, the modeling near the wall will be described.

2.4.3.1 The law of the wall and y^+

Close to a wall, with the no-slip condition, a boundary layer will rise as shown in Figure 2.9. The velocity goes from zero at the wall to the free stream velocity further away from the wall. In a turbulent flow, the variations will be largest in the near wall region, and this will cause the strongest gradients to occur here. Solving the governing equations near the wall is therefore difficult due to the variations of the dependent variables, such as velocity and the wall shear stress. Since in this project it is important to capture the near wall gradients, a large number of nodes are needed.

The boundary layer near the wall consists of two layers:

1. Viscous sublayer, $y^+ < 5$. A thin layer next to the wall where viscosity has a greater influence since the flow on average behaves close to laminar. In the viscous sublayer;

$$y^+ = u^+$$
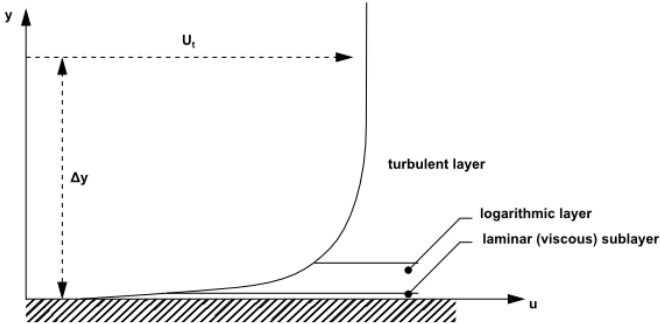
Figure 2.9: Boundary layers near wall

2. Logarithmic layer is the region between the viscous sublayer and the fully turbulent layer. Here where the mixing turbulence is the dominant variable, with $60<y^+<200$. In this layer, u^+ is proportional with ln (y^+). This relation is called the law of the wall, see equation (2.22). In between these two layers, $5<y^+<60$, there is a region called the buffer layer. Here, the flow is still dominant of viscous effects, but turbulence are becoming significant.

In ANSYS Fluent there are two approaches to model the near-wall region;

1. One approach is using semi-empirical formulas called wall functions to bridge the region between the wall and the fully-turbulent region. This means that the region covering the viscos

region and the buffer layer is not resolved. The advantage using this method is that a coarse mesh can be used to model high gradient shear layers near the wall, and this will save computational cost by saving CPU time and storage.

2. In the other approach, the turbulence models are modified to resolve the viscosity-affected region close to the wall. This requires a fine mesh into the viscous sublayer (ANSYS Fluent, 2013, 4.14.1.1.). This second method is known as the low Reynolds number method. Turbulence models based on the ω-equation are suitable for low Reynolds, like the SST as will be explain later. This method requires higher computational power than the wall function, since more storage and runtime is required.

The standard wall functions in Fluent is an extension of the Launder-Spalding method, which involves the following steps (Bredberg, 2000, pp. 11-12):

1. Solve the momentum equation with a modified wall viscosity.

2. Solve the turbulent kinetic energy, with modified integrated production and dissipation terms.

3. Set epsilon using the predicted *k*.

The logarithmic law of the wall for the mean velocity parallel to the wall is defined as;

$$u^+ = \frac{U_t}{u_\tau} = \frac{1}{k}\ln\left(y^+\right) + B \tag{2.22}$$

where

$$y^+ = \frac{\rho \cdot y \cdot u_\tau}{\mu} \tag{2.23}$$

and,

$$u_\tau = \left(\frac{\tau_\omega}{\rho}\right)^{1/2} \tag{2.24}$$

where,
u^+ is the near wall velocity
u_τ is the skin friction velocity
U_t is the known velocity tangent to the wall at a distance of Δy from the wall

y^+ is the dimensionless distance from the wall

τ_ω is the wall shear stress

κ is the von Karman constant

B is the log layer constant depending on the wall roughness.

In Figure 2.10, the law of the wall and the logarithmic-law is compared.
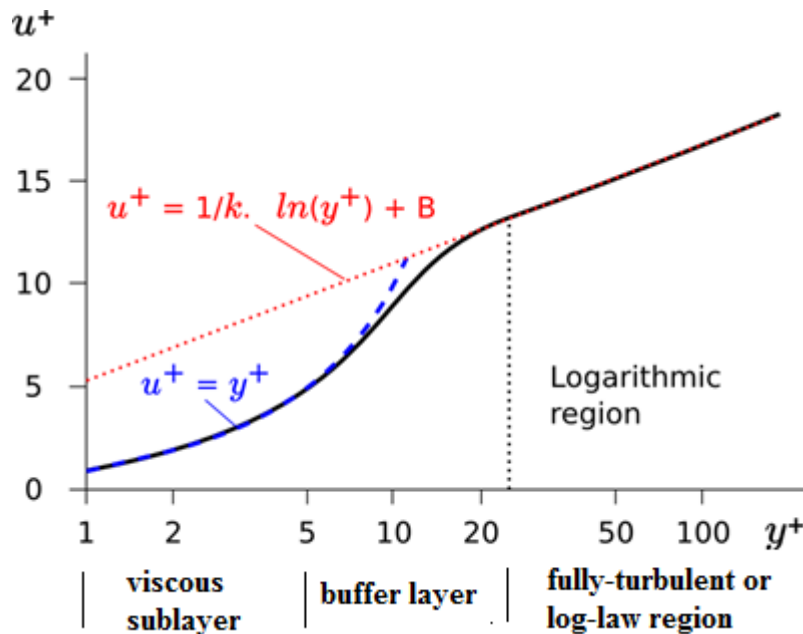
Figure 2.10: The law of the wall.

Equation (2.22) has a downside becoming singular at separation points where the near wall velocity approaches zero, therefore a scalable wall-function is needed. This function uses an alternative velocity scale, u^* instead of u_τ. The standard wall function gets weak when the mesh is refined, and then the scalable function can be applied on arbitrarily fine mesh and allows performing a consistent mesh refinement independent of the Reynolds number (ANSYS Fluent, 2013, 4.14.3.).

The dimensionless distance from the wall, y^+ is important in CFD because it is important to know the location of the first node away from the wall.

2.4.3.2 k-ϵ turbulence model

This is a two-equation model within the RANS models, which means that two transport equation needs to be solved, one for the turbulent kinetic energy, k, and one for the turbulent dissipation, ϵ, which is the rate of dissipation of k.

The k-ϵ model is well tested and the most widely used turbulence model. It is known to be successful solving a wide variety of industrial relevant flows without changing the model constants. It is particularly well in confined flows where the Reynolds shear stresses are most

important.

Limitations for the model are weak shear layers, Boundary layer separation, flows over curved surfaces and rotating flows (Versteeg & Malalasekera, 1995, pp. 74-75).

In Fluent the k-ϵ uses the scalable wall-function approach to improve robustness and accuracy when the mesh close to the wall is fine, but it will not resolve the boundary conditions. By using the k-ϵ in near wall modelling, the flow is assumed to have the characteristics as a fully developed turbulent boundary layer. Instead of solving the governing equation in the first cell closest to the wall, the velocity profile is assumed to be as in the law of the wall, Figure 2.10. The usage of this scalable wall-function requires the first node from the wall to be in between $30 < y^+ < 300$. The model is not suitable for flows with separation and flow over curved surfaces.

The turbulent viscosity, μ_t, is computed by combining k and ϵ as follows (ANSYS Fluent, 2013, 4.3.1.2.):

$$\mu_t = \rho C_\mu \frac{k^2}{\varepsilon} \tag{2.25}$$

where C_μ is a constant.

2.4.3.3 k-ω and Shear Stress Transport model

When the k-ϵ model fail and the ϵ- models fail to solve the separation, other models are needed to model the flow. The most prominent two-equation model in this area is the k-ω model. Compared to the k-ϵ, this model does not involve the complex damping functions if it gets integrated down to the viscous sublayer. By solving the low Reynolds number method, this model is a preferred choice when it comes to near wall treatment. A low-Reynolds number k-ω requires at least $y^+ < 5$. The model assumes that turbulence viscosity, μ_t, is linked to turbulent kinetic energy k_e, and turbulent frequency, ω, via the relation (ANSYS Fluent, 2013, 4.4.1.3.):

$$\mu_t = \alpha^* \frac{\rho k}{\omega} \tag{2.26}$$

With the coefficient, α^*, as a damping of the turbulence viscosity causing a low-Reynolds number correction.

The k-ω model is used in another model called the Shear Stress Transport (SST) model. It accounts for, as from the name, the transport of turbulent shear stress. It is designed to give a more accurate prediction of the onset and the amount of flow separation under adverse pressure gradients.

The SST model in Fluent is using an automatic near-wall treatment by applying both the wall-function and the low-Reynolds number approach. This is done by using the k-ε for the free-stream and the k-ω for at the viscous sublayer. The model is similar to the k-ω but includes the following refinements (ANSYS Fluent, 4.4.2.1.):

- The standard k-ω model and a transformed k-ε model are both multiplied by a blending function and added together. The blending function is in the near-wall region which activates the k-ω model.
- The definition of the turbulent viscosity is modified to account for the transport of the turbulent shear stress.

The SST model will therefore require a $y^+ \leq 5$ and at least 10 inflation layers near the wall as for the k-ω model. Between the extremes, the SST uses a blending function to achieve a mix of the k-ε and k-ω. SST model should give the best results when the flows are separated, and should be a preferred choice of model flow including particles.

2.4.3.4 Wall Interactions

With different particle impacts on the wall along a pipe, it is important do go into how a CFD code is treating this. Particles are transferring kinetic energy to the wall when hitting it. The velocity after the particle-wall collision is dependent on the particle properties, the wall material and the fluid phase. In Fluent, the restitution coefficient is providing this information when the boundary condition for the wall is set to *reflect* the particles. This factor or coefficient defines the amount of momentum, in the direction normal to the wall, which is retained after the collision with the wall (ANSYS Fluent, 2013, 24.4.1.):

$$e_n = \frac{v_{2,n}}{v_{1,n}} \tag{2.27}$$

Figure 2.11 show the "reflect" boundary condition for the discrete phase:
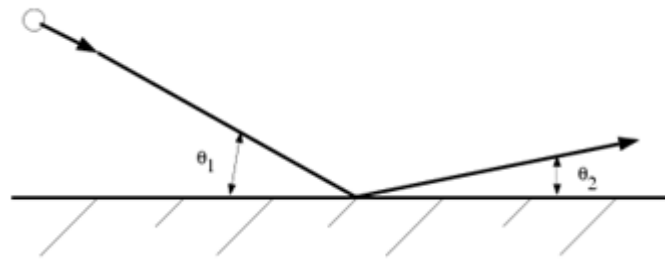
Figure 2.11: «Reflect» boundary condition for the discrete phase (ANSYS Fluent, 2013, 24.4.1)

This means that a restitution effect of 1.0 implies that the particle retains all its kinetic energy after the rebound, and the collision is elastic. If it is less than 1.0, the collision is inelastic and the kinetic energy of the particle is less than before the impact.

Particles may also in some cases stick to the wall or remain very close to the wall after hitting it. For these situations, special boundary condition need to be developed. A tangential or normal coefficient of restitution equal to 0.0 implies that the particle stick to the wall.

2.3.5   Multiphase flow modeling

Multiphase flow is defined as a fluid flow consisting of more than one face or component. In this thesis, where sand particles are transported with the fluid through a pipe, the simulation have to be handled as a multiphase flow simulation.

Multiphase flow can be classified into three different groups:

> 1. Dispersed flows: Particles, bubbles or droplets in the liquid.
>
> 2. Intermittent flow: Slug and annular flow as a gas-liquid mixture.
>
> 3. Separated flow: liquid and gases.

Currently, there are two different types of approaches for numerical calculation of multiphase flow. They will be described in the following chapters and are based on these descriptions;

Lagrangian description will track the position and velocity of a small number of particles through the continuum fluid. The motion of an individual particle is based on the Newton's laws. The advantage using the Lagrangian method is that it is very useful describing particles behavior.

27

Eulerian description will define a control volume or a flow domain. It is possible to describe the flow properties at every point in space as time varies. This way of looking at the motion of the fluid is by focusing on the specific location in the domain where the fluid flows as time passes.

2.3.5.1 Lagrangian Discrete Phase Model

The Lagrangian Discrete Phase Model (DPM) in ANSYS Fluent follows the Euler-Lagrange approach. As a rule of thumb, particle concentration should be less than 10 vol% for this approach for the model to work. The fluid is treated as a continuum by solving the time-averaged Navier-Stokes equations. When the fluid is solved correctly, a large number of particles are tracked through the field. When doing this, the particles are transported through the fluid without affecting the fluid and without taking up any volume since this is neglected. Therefore, also particle-particle interactions can be neglected (ANSYS Fluent, 2013, 16.1.1.). With this fixed continuous phase, it is said to be a *one-way coupling* between the phases. It is though possible to incorporate the effect of the discrete phase on the continuum and achieve a *two-way coupling* between the phases. This is accomplished by alternately solve the discrete and continuous phase equations until the solutions in both phases have stopped changing (ANSYS Fluent, 2013, 16.13.1.). Illustration in Figure 2.12:
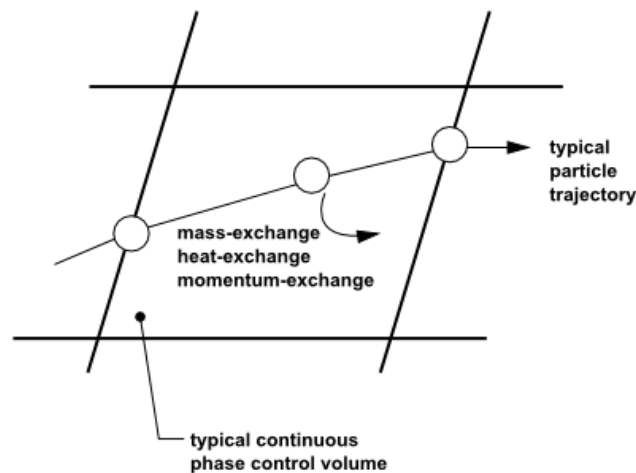
*Figure 2.12: Heat- mass- and momentum transfer
between the discrete and continuous phases*

In Fluent, the particle trajectories are computed individually at specified intervals during the fluid phase calculations. This is done by integrating the force balance on the particle as described in chapter 2.3.3, which is written in a Lagrangian reference frame.

When simulating particle trajectories, the specified boundary condition needs to be set. The most important boundary conditions are the one for the walls, which should represent a collision between the particle and the wall. In this thesis, the erosion model used for the Lagrangian approach, and later within the Eulerian model, is the DNV erosion model. This model is not available in ANSYS Fluent, and has to be implemented manually. Particle erosion and accretion rates can be monitored at wall boundaries and is calculated from the relationship shown in chapter 2.2.1 in equation 2.5. The varying factor is the angle where the particles strike the wall. This impact angle function has to be defined in the wall boundary under the Discrete Phase Model (DPM) tab. For the DNV model, this impact angle function is the blue line in Figure 2.6 in chapter 2.2.1, since ductile materials are used in this thesis. This function is implemented by using 15 points along the line, and it is added as a pricewise-linear fit.

It is also important to define both the diameter function, K and the velocity exponent function, n in the equation, which is the material constants. The recommended values for steel are given in Table 2.4 in chapter 2.2.1.

2.3.5.2 Discrete Element Method

A model that need to be described is the Discrete Element Method (DEM) which is based on the work of Cundall & Strack (1979), and accounts for the forces that result from collision between particles. The method is based on the use of explicit numerical scheme in which the interactions of the particles is monitored contact by contact and the motion of the particles are modelled particle by particle (Cundall & Strack, 1979). The discrete element method is suitable for simulations of granular flows, which are characterized by higher particle loading. DEM is usually included in simulations where particle-particle interactions are important.

The force resulting from the particle collision will come as an additional force to the equation 1.12 in chapter 2.4.3. This is determined by the deformation, which is measured as the overlap between pairs of spheres (ANSYS Fluent, 2013, 16.12.1.).

When two particles interact and bounces off each other, it can be looked at like in Figure 2.13 (ANSYS Fluent, 2013, 16.12.1).

* not to scale, greatly exaggerated
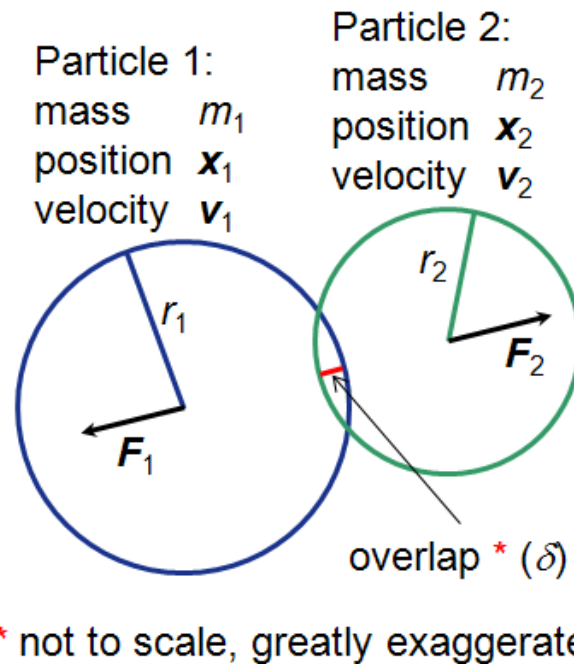
Figure 2.13: Particles represented as spheres (ANSYS Fluent, 16.12.1).

The method is based on the spring constant, k, and the size of it when particles come in contact. The value of k can be estimated from the following equation (ANSYS Fluent, 2013, 16.12.1.):

$$k = \frac{\pi v^2}{3\varepsilon_D^2} D\rho \tag{2.28}$$

where,

D is the parcel diameter, ρ is the particle mass density, v is the relative velocity between colliding particles, and ε_D is fraction of the diameter for allowable overlap.

The collision force laws used in this thesis for the DEM are:

1. The *Spring-dashpot* collision law is a linear spring force law with a dashpot and is used for the normal forces.
2. The *Friction Collision* law is based on the equation for Coulomb friction (2.7) in chapter 2.2.2. This law is used for the tangential forces.

As for the DPM, the particles in DEM are not tracked individually but as parcels of particles. Each parcel is the determined by tracing a single representative particle. The parcel approach is

used in Fluent instead of single particle tracking because the computational cost is much lower. DEM differs from DPM in following ways (ANSYS Fluent, 2013, 16.12.1.4):

- The mass used for DEM calculations of the collision is the one from the entire parcel and not just the single particle.
- The radius of the DEM parcel is a sphere and the volume is the mass of the entire parcel divided by the density of the particle.

When including the DEM collision model, the particle tracking changes to an implicit scheme, which means an implicit Euler integration of equation (2.12) which is unconditionally stable for all particle relaxation times (ANSYS Fluent, 2013, 24.2.7.1.).

2.3.5.3 Euler-Euler Approach

This approach make it possible to treat each of the different phases mathematically as interpenetrating continua. With a liquid- and solid phase present, the solids will occupy a volume, which it is not in the Lagrangian approach. This introduce the phasic volume fraction. These volume fractions are assumed to be continuous functions of space and time and their sum is equal to one. Conservation equations for each phase are derived to obtain a set of equations, which have similar structure for all phases. By providing constitutive relations that are obtained from empirical information, the equations are closed. In case of a granular flow, these are closed by application of kinetic theory (ANSYS Fluent, 2013, 17.2.1.1).

The simulations are said to be fully coupled, since the different phases interact with each other, particle-particle interaction occur and the particles take up volume in the flow. This particle to particle interaction will then come into play in both typical elastic particle-particle interaction as well as grinding viscous interaction between particles. These interactions, and the turbulence affecting the near-wall velocity, permits the particle to strike the wall at random impacts and particle impact erosion occurs. Different patterns of solids in the flow can be observed depending on the nature of the slurry and the flow conditions.

For denser slurries, with high particle concentration, a CFD simulation using this approach should give the best results and give most reliable results. Within the Euler-Euler approach, there are three different models available in Fluent. *The Volume of fluid* (VOF) model, the *Mixture Model* and the *Eulerian Model*.

In this thesis, the model described and chosen is the Eulerian multiphase model. This model also includes the Eulerian parameter, the Dense Discrete Phase Model (DDPM).

Eulerian Model with Dense Discrete Phase Model

The Eulerian model make it possible to model multiple separate, but with interacting phases. Simulations with almost any type of combinations of solid-, liquid- and gas-phases can be performed where an Eulerian approach is used for each phase. With this possibility of modeling different phases, the only limitation is the memory requirements and convergence behavior. This model is the most complex of the multiphase models, and therefore it is difficult to get a converged solution (ANSYS Fluent, 2013, 17.15.1.).

The Eulerian model in Fluent is based on the following (ANSYS Fluent, 2013, 17.15.1.)

- A single pressure is shared by all phases
- Momentum and continuity equations are solved for each phase
- For a granular phase:
    o Granular temperature can be calculated for each solid phase
    o Solid-phase shear and bulk viscosities are obtained by applying kinetic theory to granular flows.
- Several interphase drag coefficient functions are available for different types of multiphase regimes.
- All the k-ε and k-ω turbulence models are available and can be applied to all phases of mixtures.

The *limitations* of the Eulerian Model relevant for this thesis are the following (ANSYS Fluent, 2013, 17.5.2.):

- The Lagrangian particle tracking which is possible to combine with the model interacts only with the primary phase. This DPM cannot be used with the model if the shared memory option is enabled.
- The Reynold Stress turbulence model is not available per phase basis.

The Eulerian Model is using a concept of phasic volume fractions to describe the different present phases. Volume fractions represents the space occupied by each of the phases, and the laws of conservation of mass and momentum are satisfied by each phase individually (ANSYS Fluent, 2013, 17.5.3.).

In this thesis, focusing on erosion and flow with particles, the *Dense Discrete Phase Model (DDPM)* is included as an Eulerian parameter in the Eulerian Model. The DPM model as described in chapter 2.3.5.1 includes the assumption that the volume fraction of the particles are sufficiently low and are therefore neglected. In order to overcome this limitation of the Lagrangian multiphase model, the volume fraction of the particle phase is accounted for in the DDPM by extending the mass and momentum equations to the following equations. (ANSYS Fluent, 17.5.18.).

This means that the DPM model is included within the DDPM while the particles takes up a volume in the fluid. This model is capturing the abrasive wear from the particles sliding along the wall by use of the wall shear stress and the solid phase velocity close to the wall. Particle-particle interactions and volume fraction of solids are captured, and also the impacts of particles also is included with the Lagrangian particle tracking.

The solid stresses acting on particles in a dense flow is modelled in Fluent by an additional acceleration, $\vec{F}_{interaction}$, in the particle force balance from chapter 2.3.3. This addition is resulting from inter-particle interaction (ANSYS Fluent, 2013, 17.5.18.2.):

$$\frac{d\vec{u}_p}{dt} = F_D(\vec{u} - \vec{u}_p) + \frac{\vec{g}(\rho_p - \rho)}{\rho_p} + \vec{F} + \vec{F}_{interaction} \qquad (2.29)$$

The additional term is computed from the stress tensor given by the kinetic theory of granular flows as:

$$\vec{F}_{interaction} = -\frac{1}{\rho_P} \nabla \cdot \overline{\tau}_s \qquad (2.30)$$

2.3.6 Verification and validation

In CFD modeling, it is essential to be aware of the quality and uncertainties the results contain, and therefore be critical for them to be used. Verification and validation are two processes for assessing the credibility of the CFD results.

Verification is defined as (Slater, 2008):

> *The process of determining a model implementation accurately represents the developer's conceptual description of the model and the solution to the model.*

Verification assessment gives an indication if the computational models are the correct implementation of the conceptual models. It will also examine if the code can be used for further analysis based on the accuracy of the result. The different ways of doing this is to verify the code, the iterative convergence, the consistency, the grid convergence and temporal convergence (Slater, 2008).

Validation is defined as:

> *The process of determining the degree to which a model is an accurate representation of the real world.*

This includes comparing the CFD results with experimental data or to the results from a Direct Numerical Solution if possible. In that case, it will only be possible to validate the code within the range where there is experimental date available.

3. CFD Analysis in ANSYS Fluent

The simulations in this thesis are rather complex and requires both a lot of memory and time to perform. Because of this complexity, a lot of different simulations, with different mesh and setups, have been performed to get best possible results. The simulation strategy and the different procedures have been performed as presented in Table 3.1.

Number	Multiphase Approach	Multiphase Parameter	Erosion Model	Geometry
1	Lagrangian	DPM	DNV	Bean Choke
2	Eulerian	DDPM	DNV+Abrasive	Straight-pipe
3	Eulerian	DDPM	DNV+Abrasive	Bean Choke
4	Lagrangian + Eulerian	DEM	DNV+Abrasive	Bean Choke

Table 3.1: Overview of simulations

In order to present the results in an organized and clear way, this chapter is describing the setup for the different simulations from the table in three different sections:

3.1: Validation of the DNV impact based erosion model against the *Bean Choke* experiment using the DPM in Fluent, *(Number 1)*. This chapter provides information about the setup for the simulation, implementation of the DNV erosion model and post-processing.

3.2: Simulation with the Eulerian model with DDPM is set up with the straight pipe case from University of Alberta as a basis, *(Number 2)*. With reliable results regarding the flow-field in the straight pipe, the same setup is used on the Bean Choke case in order to include the abrasive wear *(Number 3)*. Several simulations are performed on the Bean Choke with different particle concentrations and erosion rate calculations are explained.

3.3: The DEM collision model are included in simulation *(Number 1)* and (N*umber 3)* in order to see the effect of the collision model on both a Lagrangian and Eulerian approach. Same procedure as the simulations, but with the DEM collision model activated, *(Number 4)*.

3.1 Validation of the DNV erosion model

Simulations have been performed in this thesis in order to validate the impact based erosion model from DNV using Fluent *(Number 1)*, against experimental results (Huser & Kvernvold, 1998, pp. 5-6). It is important to get the DNV erosion model validated against an experimental case since it is used as a part of the DDPM within the Eulerian model later in the thesis *(Number 2 & 3)*.

The simulation method used in this case has been as follows:

1. Replicate geometry from experiment and generate a suitable mesh.
2. Solving the fluid on a fine mesh.
3. With a converged simulation result of the fluid, particles are released at the inlet and tracked through the domain without re-solving the fluid. The particles are then defined as one-way coupled to the fluid.
4. Erosion rate is calculated and compared with experimental results.

3.1.1   Geometry and meshing

The bean choke case from DNV is chosen as a validation case. A carbon-dioxide gas at subsonic speed, containing sand particles, is flowing through a contraction as shown in chapter 2.2.3.

DesignModeler in ANSYS has been used to model the bean choke. The geometry have been sketched in 2D and then a *revolve* function has been used to make the 3D Bean Choke.

Several attempts have been made using the *ANSYS Meshing* to mesh the domain. ANSYS Meshing was not able to get converged solutions with sufficiently small first layer thicknesses. The different meshes from ANSYS Meshing tested on the case have not been used for any further results in this thesis, but the attempted methods is described briefly in *Appendix A*.

Because of the divergence problem with ANSYS meshing, another program was chosen. *ANSA meshing* reported very good mesh quality with a $y^+ < 5$, which is suitable for the k-ω SST turbulence model. The *ANSA* mesh used for all the Bean Choke simulations is shown in Figure 3.1 and the mesh-info in Table 3.2.
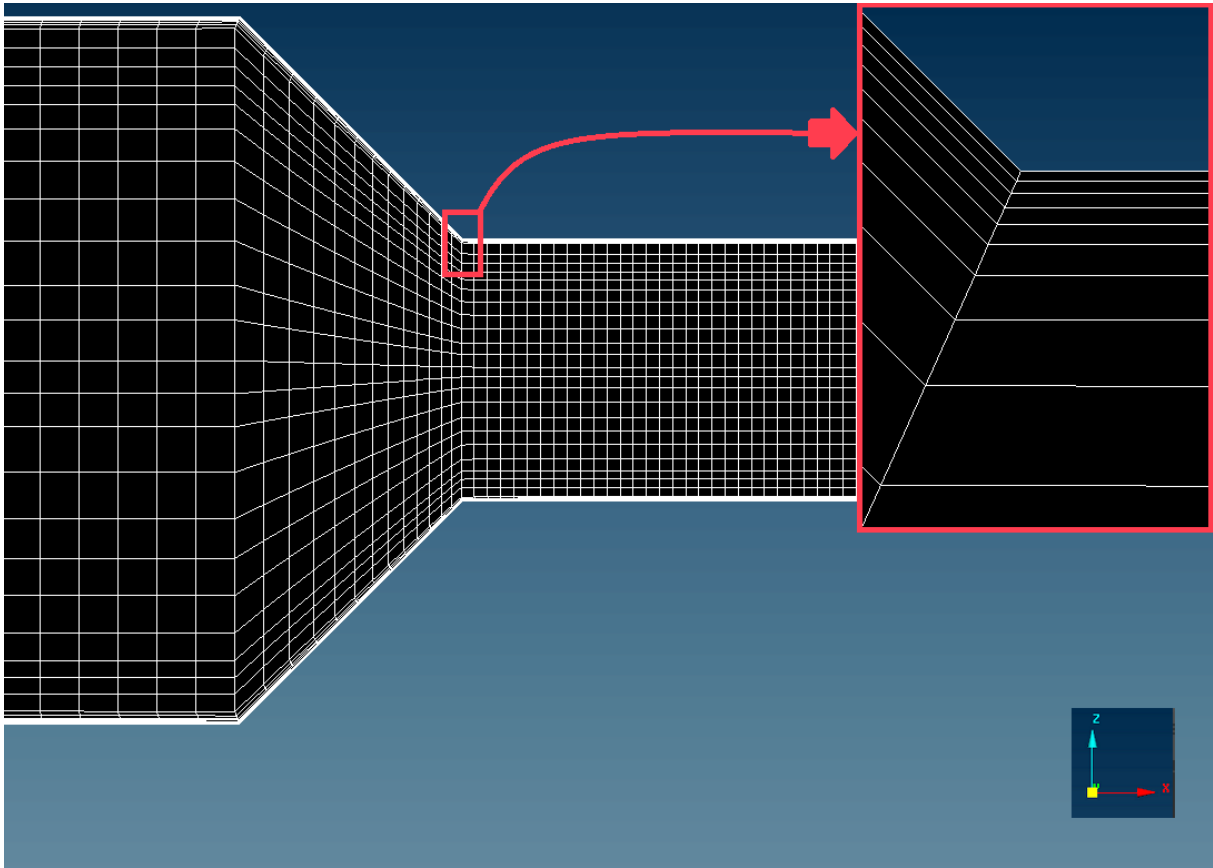
Figure 3.1: ANSA-mesh with thin inflation layers

	ANSA-mesh
Nr. of elements	1293012
Nr. of nodes	1012186
Element size [mm]	1.0
First layer thickness [mm]	0.0001
y^+	3.5565

Table 3.2: Mesh-info for the chosen grids.

Several simulations with different meshes have been performed on the Bean Choke in order to develop the final mesh. The main focus have been on the y^+ value since this is important for the fluid simulation.

3.1.2 Pre-process

The simulation has been set up in ANSYS Fluent as a steady state simulation with a SIMPLE Solution Method. The flow and particle parameters from the validation case by DNV are given in Table 3.3 – 3.4. More details about the setup, see *Appendix B* for the Fluent input summary.

In order to get a good solution close to the wall, and with the $y^+ < 5$, the k-ω SST is preferred as turbulence model for the fluid simulation. As described in chapter 2.4.3.3, this turbulence model will use the k-Ω when y^+ is less than 5, k-ε if larger than 30. In-between these y^+ values, a blending function is used which is a mixture of the two models.

First, the simulation of the fluid is performed without the DPM activated, and with the fluid parameters as listed in Table 3.3:

Fluid	Carbon-dioxide
Thermal	None
Turbulence model	k-ω SST
Wall functions	Automatic
Inlet velocity	11.4 [m/s]
Fluid viscosity	1.5e-5 [kg/ms]
Outlet relative pressure	0
Wall Boundary	No slip, smooth walls

Table 3.3: Fluid Parameters

With a sufficiently good result of the fluid, and a solution close to the wall, the DPM is activated and particles are released at the inlet, without resolving the fluid.

Particle parameters, DPM setup and wall boundary conditions is listed in Table 3.4:

Particle diameter	0.25 mm
Particle density	2600 [kg/m]
Sand particle definition	Medium Coarse
Particle coupling	One-way
Mass flow	0.000164 [kg/s]
Erosion Model	Det Norske Veritas (DNV)
Diameter function, K	2e-09
Velocity exponent function, n	2.6
Normal reflection coefficient	0.8
Tangent reflection coefficient	1
Drag law	Morsi and Alexander
Virtual mass force	None
Particle collision	None

Pressure gradient force	Yes
Particle breakup	No
Scale flow rate by face area	Yes

Table 3.4: Particle parameters

The erosion model used for this simulation is the DNV erosion model which is implemented to ANSYS Fluent manually as described in chapter 2.3.5.1.

3.1.3   Particle tracking and Post processing

The simulations have been post processed in ANSYS Fluent. After first solving the fluid, the results are post-processed to make sure that the solution is good.

The particles are then injected at the inlet and tracked through the domain. When this process is done, it is possible to display the erosion rate results on a contour. The results regarding erosion rate reported by Fluent, (*DPM_erosion_rate*) are given in [kg/m^2-s], while the experimental results are using [μm/kg$_{sand}$]. A user defined parameter is therefore defined in Fluent in order to convert the ER to the same unit:

$$ER_{impact}\left[\mu m / kg\right] = \frac{(DPM\_erosion\_rate)\cdot 10^6}{(7800\cdot 0.000164)} \tag{3.1}$$

where 7800 is the wall material, steel, with density in [kg/m^3] and 0.000164 is the particle mass flow rate given in [kg$_{sand}$/s].

The erosion rate results along the wall after the contraction are written to file and implemented into an Excel file. A Matlab script read these results and plot them against the experimental results.

3.2 Eulerian Model with DDPM

The Eulerian model with DDPM is first tested on the straight pipe geometry from University of Alberta *(Number 2),* since this is a simple geometry with only a straight pipe, which makes it easier to set up the complex simulation. As described in the experimental paper, erosion should be visible at the bottom pipe wall due to gravitational forces acting on the particles. With a particle concentration of 13.5 vol %, which classifies the flow as a *dense slurry* as described in chapter 2.1.1.

With reliable results from the straight pipe, the same Eulerian model with DDPM setup should be tested against the *Bean Choke* experiment to see how the addition of abrasive wear affects the result *(Number 3)*.

3.2.1 Geometry and meshing

A straight pipe is created in *DesignModele*r with a long inlet length to be sure to get fully developed flow in the pipe. Mesh is created in *ANSYS meshing*. With this simple geometry, a sweep method is used along the pipe, with thin inflation layers in order to get a good solution close to the wall. The mesh is a hexa-mesh, and is shown in Figure 3.3.
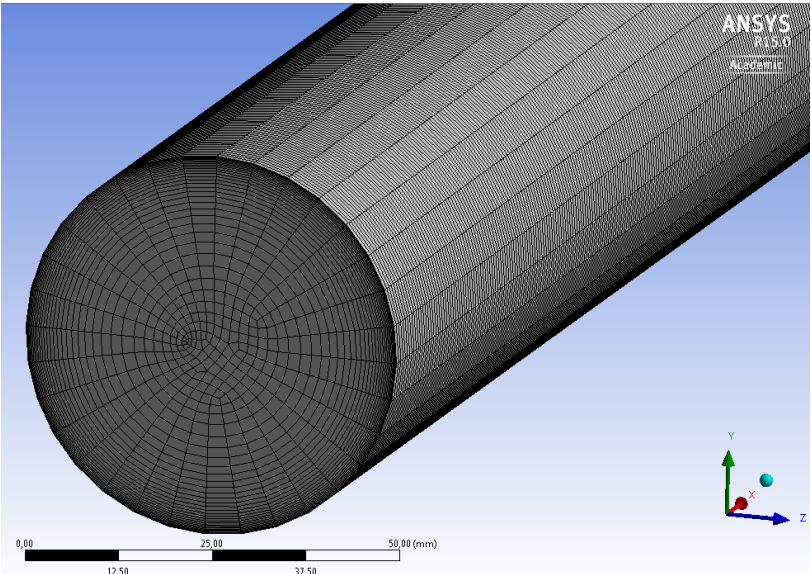
Figure 3.2: Hex-mesh used for the straight pipe simulation.

The mesh info is listen in Table 3.5.

Nr. of elements	1026000
Nr. of nodes	1044043
Element size [mm]	5
First layer thickness [mm]	0.1
Aspect ratio	13.57
y^+	8.7065

Table 3.5 Mesh info

For this simulation *(Number 2)*, *ANSYS Meshing* reports good quality and no signs of divergence in the solution. Therefore, the ANSA Meshing program have not been tested for this simulation.

3.2.2 Pre-process

The Eulerian model with the DDPM is set up in ANSYS Fluent. For this fully coupled multiphase simulation, three models have to be activated in Fluent;

1. Multiphase model is set to Eulerian and the DDPM chosen as Eulerian parameter. This automatically includes one discrete phase.
2. The Viscous model is set to the k-ε turbulence model since the flow through the pipe is turbulent. The k-ω SST is not chosen in this simulation since $y^+ > 5$, i.e. the k -ω is not necessary. Choosing the k-ε turbulence model will also simplify the already complex simulation.
3. DPM turns on automatically when choosing the DDPM as the Eulerian parameter.

The next step is to define the two phases; one primary phase of continuous fluid and one discrete phase. Boundary conditions are then set at inlet, walls and outlet. For inlet conditions, it has to be specified mass flow for the continuous phase and then a pressure condition for the mixture. Outlet condition is zero relative pressure. At the walls, the DNV erosion model is implemented as in the bean choke simulation, since this simulation also includes the DPM.

The solution method used in this simulation is the Phase Coupled SIMPLE scheme. Table 3.6 list the important parameters used in the simulation.

	Fluid	Water
Fluid	Fluid viscosity	1.003e-3 [kg/ms]
	Fluid density	998.2 [kg/m^3]
	Solid	Sand
	Density	2600 [kg/m^3]
Solid particle	Diameter	1.5 [mm]
	Volume fraction particles	0.1338262 [-]
	Sand particle definition	Coarse
Multiphase model	Multiphase model	Eulerian
	Eulerian parameter	DDPM
Turbulence model	Turbulence model	Realizable k-ε
	Wall functions	Standard

	Discrete phase model	On
	Update DPM source	Every 30 iteration
Discrete Phase Model	Virtual mass force	Yes
	Pressure gradient force	Yes
	Drag force	Morsi and Alexander
	Scale flow rate by face area	Yes
	Inlet mass flow	7 [kg/s]
	Outlet relative pressure	0 [Pa]
Boundary conditions	Wall Boundary	No slip, smooth walls
	Erosion model	DNV
	Solution method scheme	Phase coupled SIMPLE

Table 3.6: Important parameters used for the Eulerian DDPM simulation with DNV.

This is an Eulerian, DDPM simulation with the DNV erosion model as a boundary at the walls, see *Appendix C* for full input summary from Fluent.

In order to capture the erosion rate due to the abrasive wear from the particles, the same simulation has to be performed with a different boundary condition for the wall. Rest of the setup is the same as in Table 3.6. See boundary conditions in *Appendix D*. This needs to be done because the abrasive wear model from ANSYS have other constants for the diameter and velocity exponent functions. These abrasive correlation constants are supplied by ANSYS Fluent. ANSYS clarifies that they have worked with its users in Houston, who actually tested abrasive erosion model with their experimental data for steel and have tuned these numbers. ANSYS also claims that these constants have since been used in many test cases and it has worked fine, while comparing it with experiments. But no benchmark is available in public domain (ANSYS Fluent Support, 2015). The variables used in the model are listed in Table 3.7.

Erosion model	ANSYS abrasive wear
Diameter function, K	1.9×10^{-8}
Velocity exponent function, n	1.41
Normal reflection coefficient	0.8
Tangent reflection coefficient	1

Table 3.7: Additional parameters used for the abrasive wear simulation.

For simulation *(Number 3)*, the procedure is the same as described for the straight pipe except for the flow conditions that are different for the Bean Choke.

3.2.3 Post processing for Eulerian modeling

The fully coupled simulations with DDPM as an Eulerian parameter are also post processed in ANSYS Fluent. The erosion rate calculations are divided into two parts; one part consists of the erosion rate calculations from particles impinging the walls, the procedure are the same as with the DPM simulation in chapter 3.1.3. The other part is a calculation method that is based on the wall shear stress of particles sliding along the wall. In order to capture the abrasive wear from the slurry flow in both the straight pipe and the bean choke, another custom erosion rate function has to be defined which includes the solid wall shear stress. The function is based on ANSYS's abrasive model, but the first two variables, the constant K and particle velocity V, are included in the wall boundary condition. So, the abrasive wear addition is calculated as follows:

$$ER_{abrasive}\left[\mu m/kg\right]=\frac{\tau_{ws}\cdot(DPM\_erosion\_rate)\cdot\left(\dfrac{\alpha_s}{\alpha_{sp}}\right)\cdot10^6}{7800\left[kg/m^3\right]\cdot\dot{m}_{particles}} \tag{3.2}$$

where,

τ_{ws} is the particle wall shear stress,

(DPM_erosion_rate) is the KV^n values from the definition,

α_s is the particle volume fraction and

α_{sp} is the Packing volume fraction.

$\dot{m}_{particles}$ is the mass flowrate of particles for a given case and 7800 is the density of steel.

All these values are calculated within the simulation and the values are therefore taken straight from Fluent when this is computed. The erosion rate results are then plotted in Fluent, and written to an excel file. Then, for the bean choke simulations *(Number 3)*, both the DDPM-DNV and DDPM-Abrasive simulation results are summarized to give the total erosion rate, which is represented by equation (3.3).

$$ER_{total}\left[\mu m/kg\right]=ER_{impact}+ER_{abrasive} \tag{3.3}$$

3.3 Simulations with DEM collision model

DPM with DEM collision model:

The DEM collision model is possible to include with the DPM model even though it is suited for simulations with higher particle loading where the particle-particle interaction is more important than in the DPM simulation. In this thesis, the DEM is included in a DPM simulation to see how it effects the erosion rate results, and if the combination is possible/usable at all. A Lagrangian DPM is cheaper than an Eulerian approach, and therefore it would be interesting to investigate the possibility to include DEM in DPM simulation on both high and low particle loading.

DDPM with DEM collision model:

For the Eulerian model with DDPM, the DEM collision model is included for its purpose, which is to include the particle-particle interaction in a slurry flow with higher particle loading. This simulation requires very complex calculations and therefore require loads of memory. The computational cost is high, and to run it on a normal computer is difficult.

In both simulations above, not much had to be changed in the original setup in order to include DEM collision model. The procedure in Fluent is as follows:

1. In the Discrete Phase Model setup in Fluent, DEM is enabled under the physical models tab.
2. Fluent then requires a particle time step for the unsteady and implicit particle tracking.
3. Under DEM collision laws, the collision pairs for particle-particle and particle-wall is defined by selecting two available contact force laws which is the spring-constant, K and friction constant ε_D.
4. In the injection properties, the DEM collision partner is chosen.
5. The last part when defining DEM collision partner is within the boundary conditions at inlet, wall and outlet. DEM is chosen under DPM to the wall material as collision partner.

4. Results and Discussion

This chapter will present the results from the simulations and the general discussion about them. The simulations will be presented in the same order as in Chapter 3, and with the results as mentioned in Table 4.1:

Number	Multiphase Parameter	Erosion Model	Geometry	Result
1	DPM	DNV	Bean Choke	Erosion Rate
2	DDPM	DNV+Abrasive	Straight-pipe	Particle Distribution
3	DDPM	DNV+Abrasive	Bean Choke	Erosion Rate
4	DEM	DNV+Abrasive	Bean Choke	Erosion Rate

Table 4.1: Overview of simulations

4.1 The results from the *Bean Choke* simulation *(Number 1)* are presented, discussed and results are compared with the experimental data from the DNV paper.

4.2 The Eulerian DDPM simulation results *(Number 2)* regarding the distribution of sand particles through the straight pipe are presented and discussed. Results from the Eulerian DDPM simulation on the *Bean Choke* are presented *(Number 3)* and compared to the Lagrangian DPM simulation *(Number 1)*.

4.3 The simulations including the DEM collision model are discussed *(Number 4)*.

4.1 Validation of the DNV impact erosion model

The results for the Bean Choke case have been very dependent on the mesh quality. In order to get a converged solution, and also get reasonable erosion rate results, the different quality parameters had to be satisfied. Aspect ratio, orthogonal quality and skewness have been looked into as important factors when developing a suitable mesh for erosion simulations. It is important to state that no other mesh independency test was performed on the *Bean Choke* than making sure that y^+ values was sufficiently low, the quality was good and that the fluid solution converged. The results from the test show that the ANSA mesh give the best results for the fluid solution and then also the best result regarding erosion rate. The ANSA mesh results are therefore the ones that are presented in this thesis.

The solution of the fluid over the contraction is shown in Figure 4.1, from simulation *(Number 1)*.
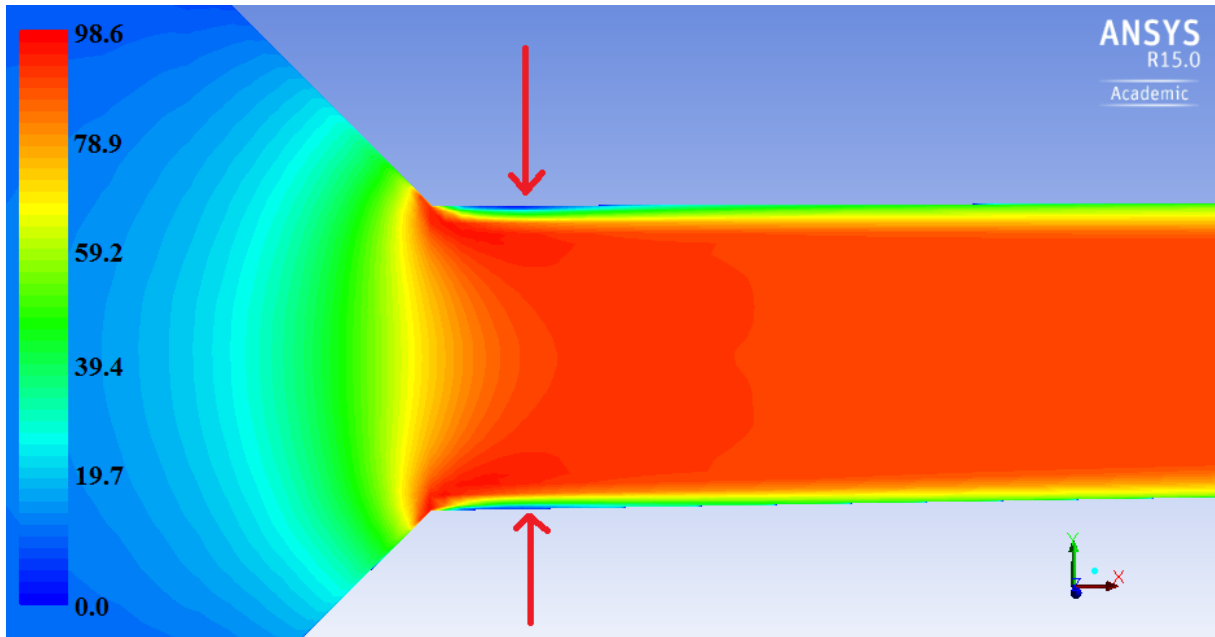
Figure 4.1: Fluid solution over the contraction.

As seen from the legend on the left side in Figure 4.1, the velocity is increasing significantly as passing through the contraction, ending up with close to 100 [m/s]. The red arrows indicates where the flow is reversed after the 45° angle increase. For this simulation, the y^+ values are sufficiently low, and less than 5. This means that the turbulence models solves the flow close to the wall. Figure 4.2 to shows the y^+ values from the simulation showing that the transition to the small pipe is the most exposed area, and is expected since this area has the highest velocity.
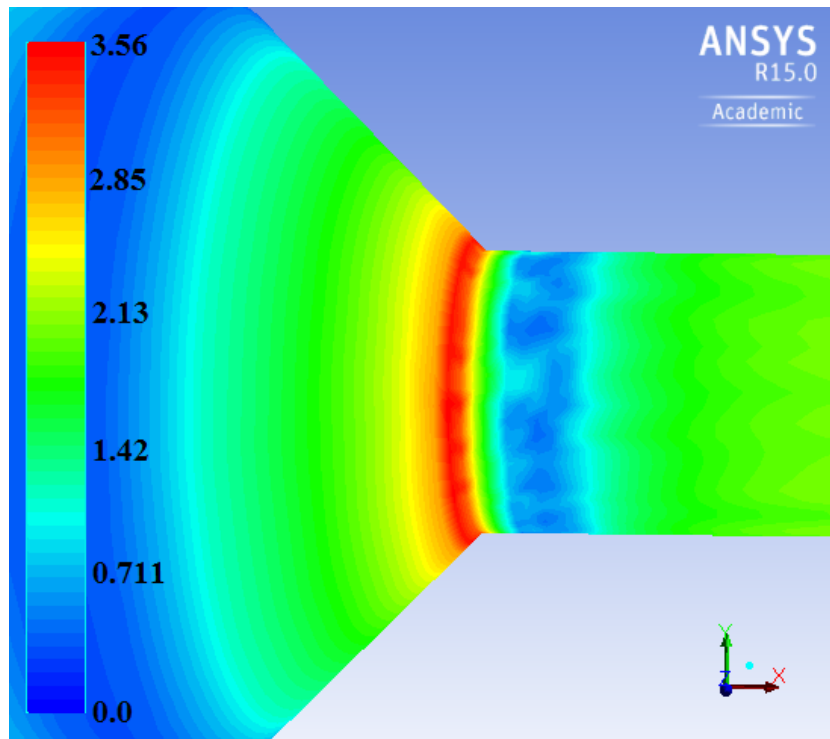
Figure 4.2: Contour of y^+ values in
the cell layer closest to the wall.

After solving the flow field, the particles are released at the inlet. The velocity profile shown in Figure 4.1 affects particles trajectories along the domain. When they are approaching the contraction, and the speed is increasing, some of them will hit the 45° wall and bounce further down the outlet pipe. Particles will also go straight through without hitting the 45° wall, as the contraction "sucks" the particles into the smaller outlet-pipe.

With these conditions, a contour of the erosion rate after the contraction is shown in Figure 4.3.
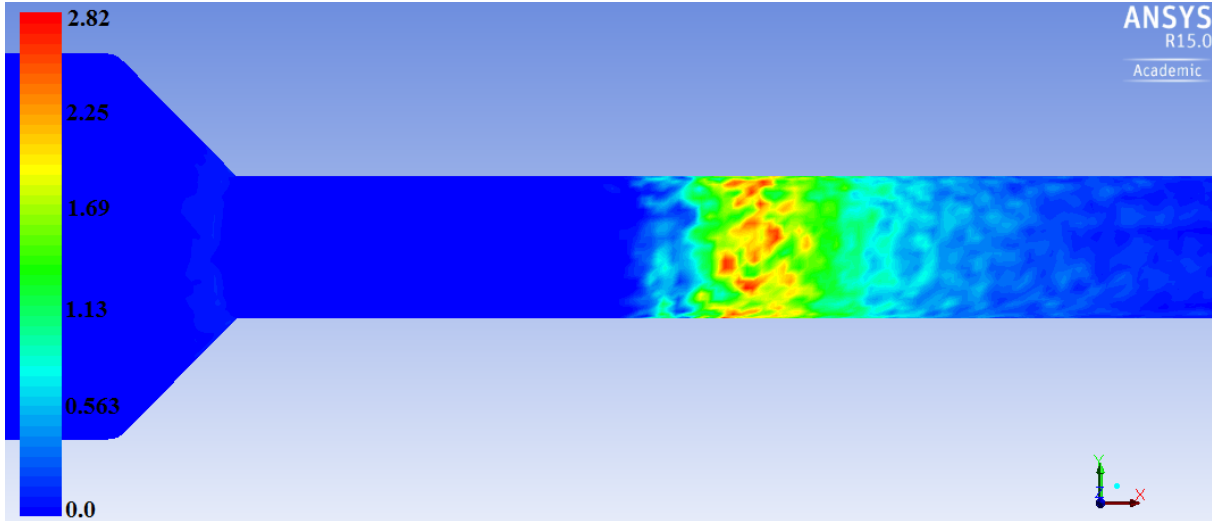
Figure 4.3: Contour of the erosion rate after the contraction, with maximum erosion.

The maximum erosion rate is located ~3.75d downstream of the outlet-pipe, and most of the erosion occur around this area. No erosion is visible in Figure 4.3 at the 45° wall before the contraction, which is because the erosion rate is lower at this point. By setting the contour range to a lower level, it is possible to see that erosion also will occur in the 45° contraction. Figure 4.4 show the erosion rate contour for the contraction part of the pipe.
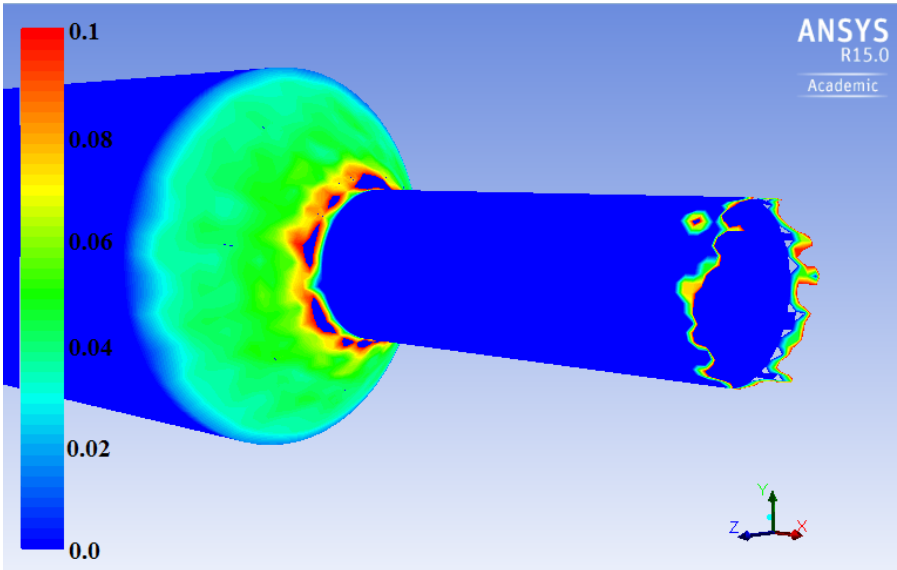
Figure 4.4: Contour of erosion rate on the 45° wall.

47

The different impact velocities for the particles can explain the different erosion rate magnitudes on the wall, which is almost ten times higher after the contraction. The impact angles are also different, and as the DNV impact function in Figure 2.6 in chapter 2.2.1 show, will the maximum erosion occur at 15°-30° (DNV, 2007, p. 12), which is the case after the contraction.

Erosion rate along the pipe section is the most important result of this simulation, since the experiment report the erosion rate from the contraction and downstream the smallest pipe. The results from the simulation are plotted against the experimental data in Figure 4.5.
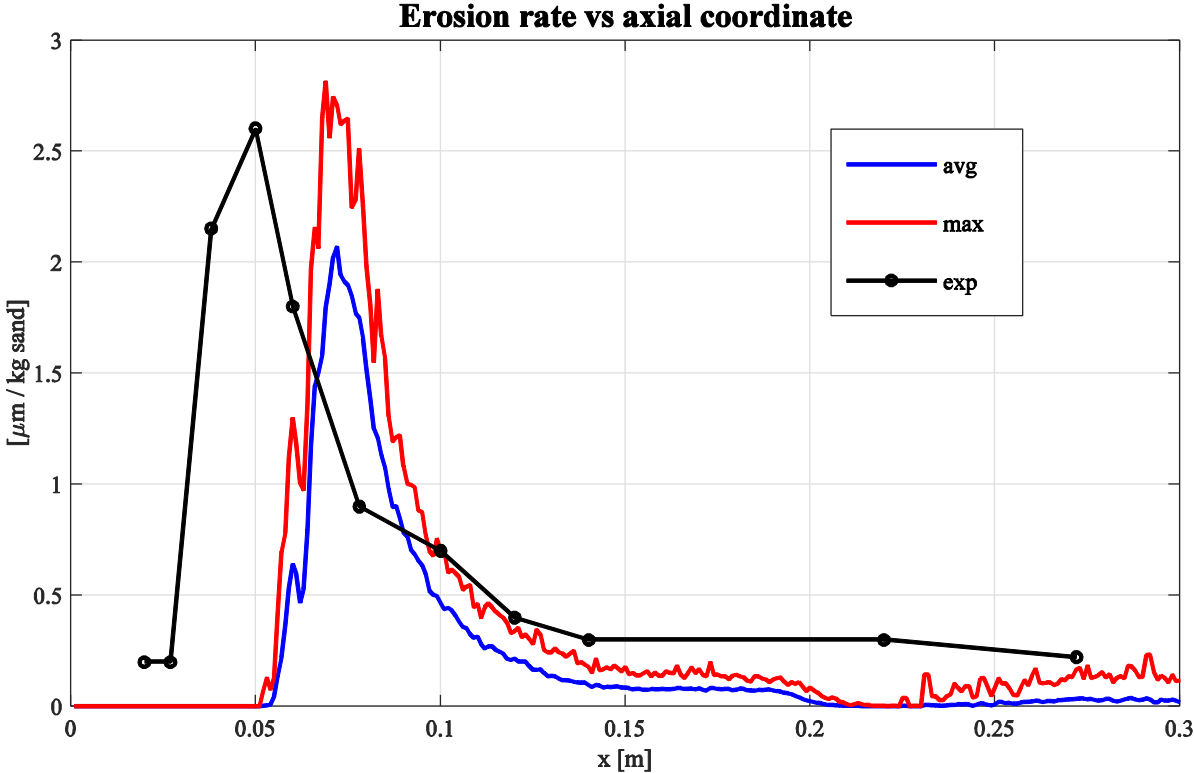
Figure 4.5: Result of the DPM simulation.

The black line represent the experimental results from DNV (Huser & Kvernvold, 1998, pp. 5-6). In the experimental paper, it is not mentioned if these values are average or maximum erosion rates, so the simulation results are presented with both the maximum (red line) and average (the blue line) values at given distance after the contraction for comparison.

Results are slightly off compared with the experiment considering the location of maximum erosion rate, which is approximately 0.02m i.e. ~1d downstream of the pipe from where the experiment registered it. The maximum average result from the simulation is a bit lower than the experiment, while the maximum show almost the same value.

Simulations have also been performed on a geometry without the sharp edge in the end of the contraction to reduce the backflow and to see how this affect the erosion rate results, and the location of the maximum erosion rate. This should reduce the swirl after the contraction, which it also does for the fluid simulation. When particles are sent through the domain, the distance from the contraction to the maximum erosion is still the same. Since the fluid affects the particles, and not the other way around with this Lagrangian approach, the particles are exposed to the swirls without affecting it. In the experiment, where the particles also affect the fluid, this swirl can be too small to have an effect on the particles flowing through the domain and therefore they hit the walls at an earlier stage than in the CFD simulations.

What the Fluent results do show, is the same erosion rate pattern as in the experiment; with one big "bump" straight after the contraction, and a slow decrease until 0.2m. After this location, the experiment registers some erosion on the pipe wall further downstream, which is not registered in the Fluent simulations. This has to do with the DPM which only capture the particles impinging the wall due to changes in flow directions etc. The model does not capture the particles sliding and jumping along the wall.

As seen in Figure 4.5, the experiment from DNV only show 11 points along the pipe where erosion rate are reported, which is few. In general, more details should have been given in the DNV paper about how and whether the geometry changed during the tests. Of course, there are many parameters that should be investigated further for the experiment, for example particle size variations, particle deformation during experiment, particle tracking with lasers etc. These parameters are not discussed in the DNV paper, and is therefore not be discussed any further in this thesis.

Simulations on the *Bean Choke* have also been performed with a two-way coupled Lagrangian approach to see if it had effect on the results. The continuous fluid is then solved while the particles are sent through the domain every 25th iteration. This means that the phases are coupled, since the particles affect the continuum in a way that they are sent through at different stages of the calculation. The result of these simulations are not any better than the one-way coupled, standard approach, and therefore not discussed any further.

4.2 Eulerian model with DDPM

With the validation of the DNV erosion model against the experimental data, the model can be used for further simulations within the Eulerian model with DDPM. In this part of the thesis, the results from the Alberta case were supposed to be used as *validation* for the Eulerian DDPM in Fluent for prediction erosion in slurry-flow systems. This is the only case found in literature that reports erosion rate results with higher particle loading. After replicating the case, and performing several simulations in order to get good results, it has come to the writer's attention that there will be a problem with the test material in the Alberta case, which is the urethane coated pipe walls. The problem is within the DPM model, which also is a part of the DDPM model; The DNV erosion model uses material constants, which are the velocity exponent function n, and the diameter coefficient, K, as, described in chapter 2.2.1 in equation 2.5. These are determined by experimental investigations, and are given for a small range of metals. The coating used in the Alberta case is urethane, which is a polymer and not a metal, and there are therefore no data in literature that can be used as material constants for this coating. Since these are very sensitive values for the erosion calculation, they have to be correct. With such a problem, the Alberta case is not suitable as a validation case when it comes to slurry erosion.

The experiment does also show results regarding the flow field and the particle distribution. With the result from the different DDPM simulations on the straight pipe experiment from Alberta, it should be possible to plot these profiles and compare the flow field from Fluent with the experiment. If this shows good agreement, the erosion rate calculation on the steel pipe should assumed to be as given. This is not a procedure to validate the Eulerian model regarding erosion prediction in the slurry flow, but an assumption that if the model can give reliable simulations of the flow-field, and an indication of how the erosion rate results will be. Due to time limitations, this procedure was not completed.

Instead the experiment was used to set up the Eulerian DDPM model by focusing on the visible wear on the bottom pipe wall, and not the magnitude. Because of the gravity affecting the high concentrated particle flow, particles are as mentioned sliding and jumping along the pipe wall. It should be possible to set up a simulation and get the erosion rate results on the bottom wall, even on a steel pipe.

With this setup for the straight pipe *(Number 2)*, Eulerian DDPM simulations are performed on the *Bean Choke* experiment from DNV in order to compare the Lagrangian DPM results with the Eulerian approach which includes the abrasive wear *(Number 3)*.

4.2.1   Straight pipe results

For the straight pipe simulation, with the same particle concentration as in the Alberta experiment, the distribution of particles over the cross-section along the pipe is shown in Figure 4.6 with particle volume fraction on the legend to the left. This figure show that particles are located close to the bottom wall due to the gravitational forces in the –Y direction acting on them, which is also the result in the experiment.
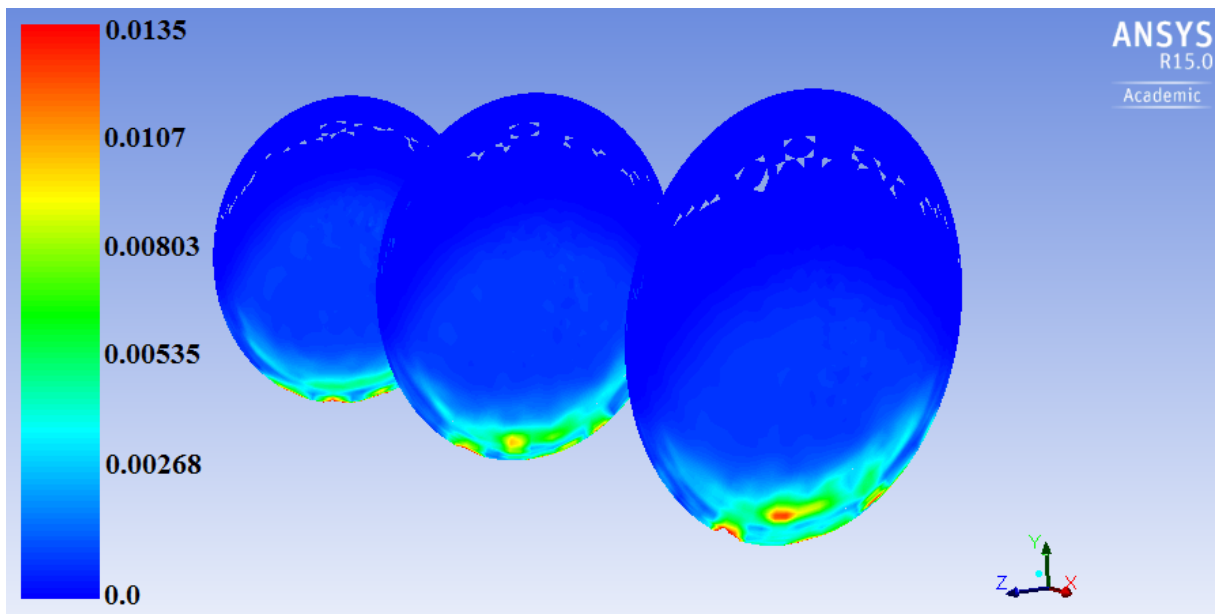
Figure 4.6: Particle distribution along the straight pipe.

This distribution of the particles are as expected when looking at the simulation results compared with the experiment (Loewen, 2013, pp. 102-108). The slurry flow in this case can be described as a settling, heterogeneous slurry flow. The momentum transfer between the particles, fluid and the walls will behave as described in chapter 2.1.3.

The wear from the sliding particles occurs at the bottom pipe wall, and the erosion rate results from Fluent is distributed as shown in Figure 4.7:
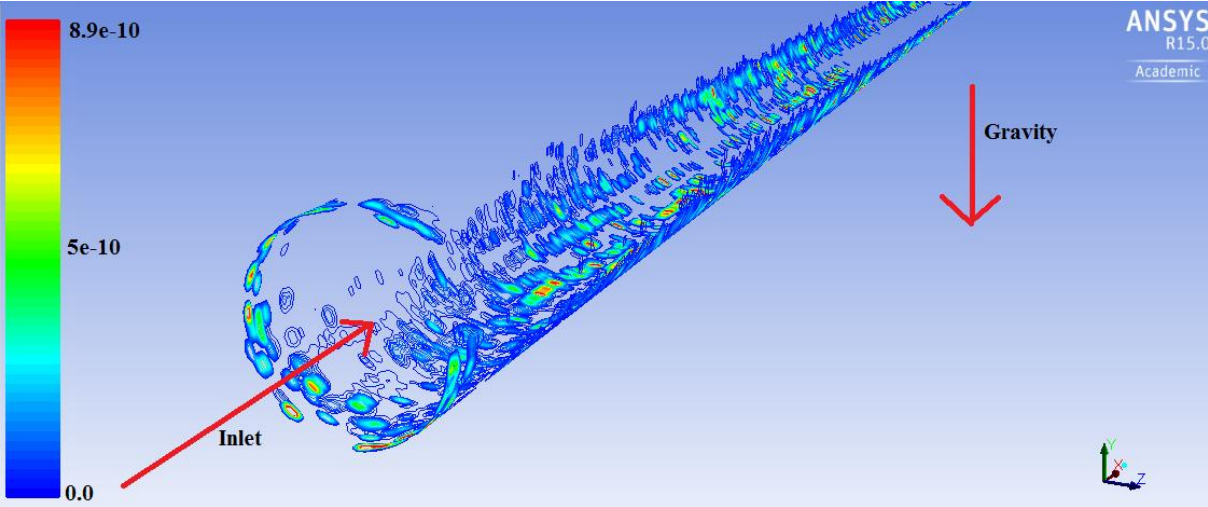
Figure 4.7: Contour of erosion rate along the pipe.

A Lagrangian DPM simulation setup was also performed on the straight pipe with high particle concentration. Results show that the pipe-walls are not exposed to erosion, which is expected from the impact based method. This is a simple geometry where the fluid do not change direction, and therefore the particles will not impact the walls and the model will not capturing the erosion.

4.2.2   Eulerian simulations on DNV's Bean Choke

After setting up the Eulerian model on the straight pipe, and starting to understand how it works, the model was tested on the Bean Choke case with different particle loadings in order to see the effect on the erosion rate when the abrasive wear becomes more dominant than at a lower level of particle loading. The DPM simulation result as discussed in chapter 4.1 is used to compare with the DDPM results with total erosion rate, and is shown in Figure 4.8 on the next page.
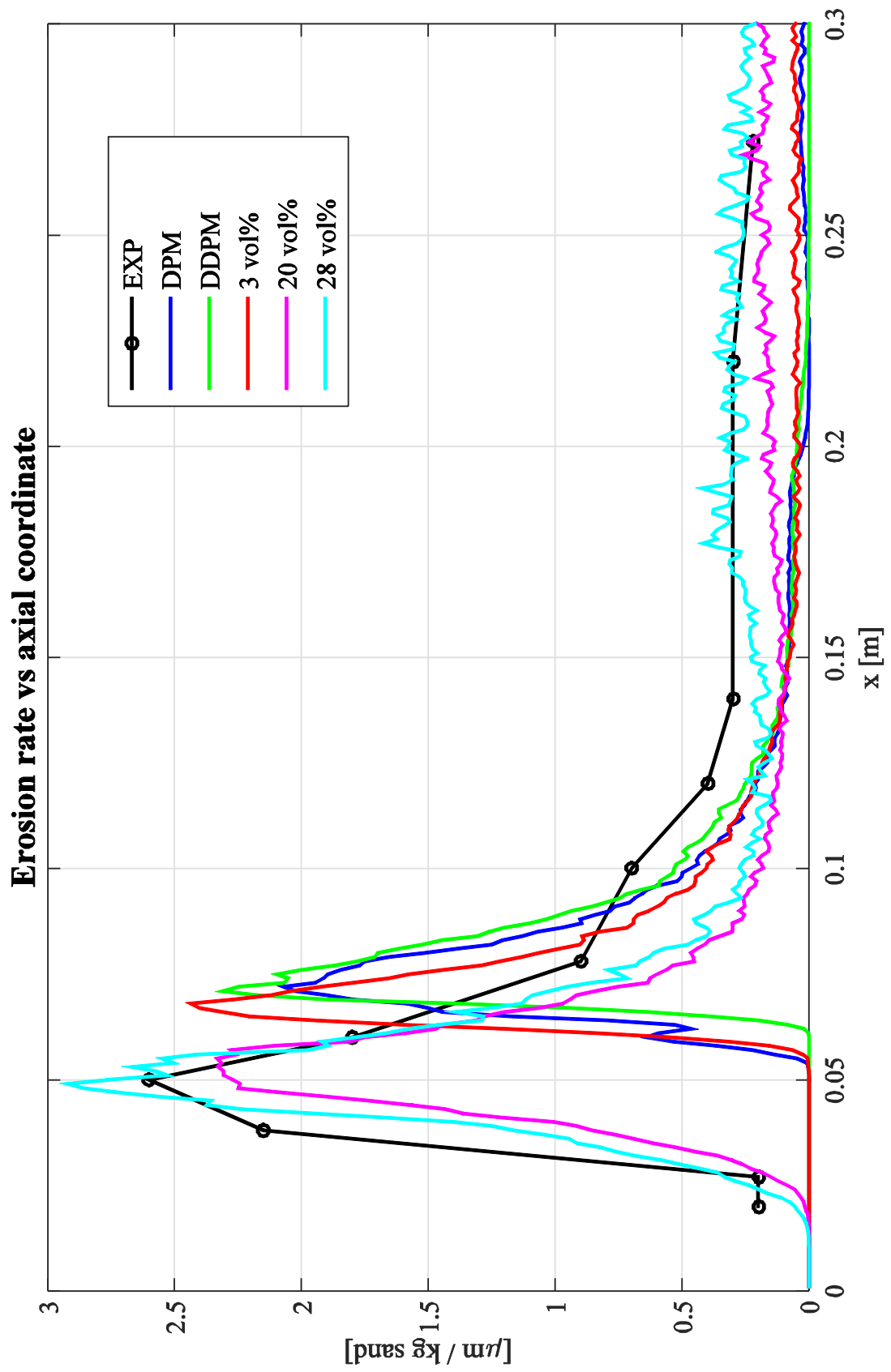
Figure 4.8: Plot of the results with different particle loading with DDPM and the DPM.

It can be seen from the plot that the DPM and DDPM, *blue* and *green*, with the same mass flow of particles gives more or less the same results. The volume fraction of particles with this mass flow is as low as 0.54 vol%, which is very low. The additional erosion rate captured from the Eulerian DDPM from particles sliding along the wall is therefore also very small as can be expected. This can also be seen further down the pipe-section, where the wear rate is as good as zero for both DPM and DDPM. The DPM neglects the volume occupied by the particles, while the Eulerian DDPM does not. By comparing the DPM *(Number 1)* with the Eulerian DDPM *(Number 3)* it is seen that the results are almost the same with this low particle loading, except for a bit higher maximum erosion rate captured by the DDPM.

As particle loading increases, it can be seen in Figure 4.8 that the maximum erosion location moves further to the left and closer to the behavior in the experimental results. This means that the maximum erosion rate occurs closer to the contraction the more particles present. This makes sense since the particle-particle interaction becomes more dominant as the particles gets pushed through the contraction and as the loading is higher, and there is less space through it. As seen on the graph, with 20 vol% and 28 vol% of particles, the erosion rate results further down the pipe are also visible and show a better agreement with the experiment. This is due to the settling particles at the bottom of the pipe, which is sliding along the wall. This shows that the higher the concentration of particles, the more dominant is the abrasive wear on the erosion rate results. The particle wall shear stress increases and is the parameter that increase the erosion rate. Erosion due to particle impact becomes less dominant.

Lagrangian DPM approach simulations were also performed with increased particle concentrations to see if the same pattern was shown with this approach. The results showed the same erosion rates on the Bean Choke, for both the magnitude and the location.

Different meshes was not tested on the DDPM simulations due to time limitations, and therefore the mesh from the DPM simulations was assumed to work with the Eulerian model.

4.3 DEM collision model

After performing both the DPM and the Eulerian DDPM simulations, the same simulations were performed with the DEM collision model activated. Several tries have been done in order to include the method but without luck. The method is a new simulation methodology, and not much is known in literature about how it works within these models. The simulations were performed on a normal computer which was very slow and after only ten iterations divergence was reported in the solution. Simulation attempts were made a High Performance Cluster in order to see if this could give any results. This also took too long, and did not give any good result within the time frame of this thesis.

5. Conclusion

In this thesis, erosion analysis were performed using ANSYS Fluent on flow containing different particle loadings. The simulation process was performed as follows:

1. The DNV erosion model was validated against an experimental case with low particle concentration. This simulation was performed by the use of the Lagrangian Discrete Phase Model (DPM) approach.

2. A Slurry flow-case simulation with the Eulerian model with a Dense Discrete Phase Model (DDPM) was set up using the flow condition results from a straight pipe experiment.

3. The same Eulerian DDPM setup was then used to simulate the Bean Choke in order to see if the model could capture the abrasive wear from the particles. All results from the above simulations were written to file, plotted in Matlab and compared with experimental results.

4. Attempts were made in order to include the DEM collision model into the erosion simulations.

Results from the DNV erosion model show good agreement with the experimental data for the Bean Choke. This model was therefore used further in the thesis within the Eulerian DDPM simulation. Even though the straight pipe could not be used as a validation case for erosion study, the Eulerian DDPM simulations show good agreement with the experiments flow conditions. The setup was then used to simulate a fully coupled Euler-Euler simulation on the Bean Choke. The abrasive wear results with the low particle concentration did not differ much from the DPM simulation. Comparing the DPM simulation *(Number 1)* with the Eulerian DDPM *(Number 3)* it is reasonable to use the Lagrangian DPM approach for cases with low particle loading. This method is cheaper when talking about computational cost, and requires less memory.

However, as the particle concentration was increased, it was evident that the Eulerian DDPM captured the abrasive wear from particles sliding and bouncing along the wall downstream the pipe after the contraction. This erosion rate could be calculated by the wall shear stress from the particles, which was increasing with the concentration.

It should be mentioned that the Eulerian DDPM is a new simulation methodology, and few investigations has so far been reported with this Eulerian parameter regarding erosion. Not even ANSYS have any validated erosion studies available with this model. Therefore, without

comparing the results from the simulations with higher particle loading with any experimental data, it is hard to draw a conclusion except from that the model capture the abrasive wear from the slurry flows as the wall shear stress from the particles increases.

When the particle concentration was increased in the DPM simulations, the results did not change much. This show that the impact based erosion models, which neglects the occupied volume of the particle, do not capture the additional abrasive erosion caused by higher particle loading, as the Eulerian DDPM do.

Several attempts were made in order to include the DEM collision model into the simulations in order to capture more of the particle-particle interactions. This method proved to be extremely memory consuming and too computational costly in order to perform on a normal computer. An attempt on a High Performance Cluster was also made but without any luck. This method is very complex and is not recommended to use for these types of simulations.

6. Recommendations for Further Work

The Eulerian model with the DDPM parameter should be validated against experimental data which gives reliable erosion rate results. More time should be spent on searching for available experimental results with higher particle concentration in literature. A suggestion would be to contact the publishers directly and get their experience with both the experiments and the available cases on the topic.

The ideal way for validation of the Eulerian DDPM model regarding erosion, would be if the same person that is doing the simulation case in CFD also performs the experiment. With this approach, it could be possible to include the effects of several important parameters to both the experiment and CFD simulations. Some of them are:

- Particle size and shape distribution
- Variation of particle loading
- Wall roughness

For the simulation part of this study, the mesh development process should be expanded in order to make sure that the results for the Eulerian simulation got mesh independent. Not much is reported in literature about how coarse or fine a mesh should be for an Eulerian fluid-particle simulation. To develop an ideal mesh can be crucial for the results.

Erosion studies, both impact based and slurry, should also be performed using different CFD programs. Both in order to compare different models in different programs, and also to look for the ideal CFD code to predict erosion.

7. References

ANSYS Fluent Support (2015).

ANSYS Help Viewer (2013). *ANSYS Help Viewer*, Verison 15.0.0.

Bredberg, J. (2000). 'On the Wall Boundary Condition for Turbulence Models', *Chalmers Internal Report 00/4*. pp. 11-12. Available at: http://www.tfd.chalmers.se/~lada/postscript_files/jonas_report_WF.pdf (29.10.2014)

Brown, N.P. & Heywood, N.I. (1991). *Slurry Handling: Design of Solid-Liquid Systems*. Essex: Elsevier Science Publishers LTD.

Cundal P.A. & Strack O.D.L. (1979). 'A Discrete Numerical model for Granular Assemblies', *Geotechnique, Vol. 29*. (no. 1), pp. 47-65. Available at: http://www.icevirtuallibrary.com/content/article/10.1680/geot.1979.29.1.47 (11.03.2015)

Det Norske Veritas. (2007). RP O501 – Revision 4.2. *Erosive Wear in Piping Systems*. Høvik: Det Norske Veritas.

Dosanjh, S. & Humphrey, J. A. C. (1985). 'The influence of turbulence on erosion by a particle-laden fluid jet', *Wear, vol. 102* (no. 4) pp. 309-330. Available at: http://www.sciencedirect.com/science/article/pii/0043164885901759 (20.03.2015)

Eltvik, M. (2013). *Sediment erosion in Francis Turbines*. Doctoral Thesis. Norwegian University of Science and Technology, Trondheim.

Gillies R. G. (1993). Pipeline flow of coarse particle slurries. Master's Thesis. University of Saskatchewan, Saskatoon. Available at: http://ecommons.usask.ca/bitstream/handle/10388/etd-03242009-142017/Gillies_Randall_G._1993.pdf?sequence=1 (15.02.2015)

Huser, A. & Kvernvold, O. (1998). *Prediction of Sand Erosion in Process and Pipe Components*. Høvik: Det Norske Veritas.

ISO 14688-1 (2002) *Geotechnical investigation and testing – Identification and classification of soil*.

King, R. P. (2002). *Introduction to Practical Fluid Flow*. Salt Lake City: Elsevier Ltd. Available at: http://www.sciencedirect.com/science/book/9780750648851 (01.04.2015)

Kosel, T.H. (1992). 'Solid Particle Erosion', *ASM Handbook, Vol. 18*, pp. 199-213. Available at: http://app.knovel.com/web/toc.v/cid:kpASMHVFL2/viewerType:toc/root_slug:asm-handbook-volume-18/url_slug:kt007PXRS6 (13.03.2015)

Loewen, D. J. (2013). *Characterization of Wear in a Laboratory-Scale Slurry Pipeline*. Master's Thesis. University of Alberta, Alberta. Available at:

https://era.library.ualberta.ca/public/view/item/uuid:5f9bcae0-1af0-4097-b62d-d4858a444938/ (18.02.2015)

Mali, T, Khudabadi, V, Rana, A.S, Vijay, A. & Adarsh, M.R. (2014). *Slurry-Flow Pressure Drop in Pipes with Modified Wasp Method*. SME Annual Meeting/Exhibit. Salt Lake City.

Meng, H.C. & Ludema, K.C. (1995). 'Wear models and predictive equations: their form and content', *Wear, vol. 181-183*, pp. 443-457. Available at: http://www.sciencedirect.com/science/article/pii/0043164895901582 (10.02.2015)

Morsi S. A. & Alexander A. J. (1972). 'An investigation of particle trajectories in two-phase flow systems', *J. Fluid Mech. Vol. 55* (part 2), pp. 193-208. Available at: http://journals.cambridge.org/download.php?file=%2FFLM%2FFLM55_02%2FS0022112072001806a.pdf&code=cf7e344ae55d4a9cb810d4d41529542f (19.04.2015)

Roitto V. (2014). *Slurry Flows in Metallurgical Process Engineering – Development of Tools and Guidelines*. Master's Thesis. Aalto University, Aalto. Available at: https://aaltodoc.aalto.fi/bitstream/handle/123456789/13113/master_Roitto_Ville_2014.pdf?sequence=1 (06.03.2015)

Shook, C. A. & Roco, M. C. (1991). *Slurry Flow: Principles and Practice*. USA: Butterworth-Henemann.

Slater, J.W. (2008). *Tutorial on CFD Verification and Validation*. Available at: http://www.grc.nasa.gov/WWW/wind/valid/tutorial/tutorial.html (15.10.2014)

Versteeg, H.K. & Malalasekera, W. (1995). *An introduction to Fluid Dynamics: The Finite Volume Method*. England: Longman Scientific & Technical.

Wasp, E. J. (1977). *Solid-liquid flow - Slurry Pipeline Transportation*. Series on Bulk Material handling Vol. 1. Germany: Trans Tech Publications.

White, F.M. (1999). *Fluid Mechanics*. Fourth Edition. Singapore: McGraw-Hill Book Co.

Wood, R.J.K, Jones, T.F, Miles, N.J. & Ganeshalingham, J. (2001). 'Upstream swirl-induction for reduction of erosion damage from slurries in pipeline bends' *Wear, vol. 25* (no. 1-12), pp. 770-778. Available at: http://www.sciencedirect.com/science/article/pii/S0043164801007153 (01.02.2015)

Zikanov, O. (2010). *Essential Computational Fluid Dynamics*. New Jersey: John Wiley & Sons, Inc.

Appendices

Appendix A

ANSYS Meshing

Several attempts were made using the *ANSYS Meshing* to mesh the domain. Two different meshing methods with the ANSYS meshing methods were used; the sweep method, which is a hex-mesh, and the tetra-mesh method:

1. The sweep method have an advantage that it is easy to keep control of the number of cells in each section along the pipe with a structured hex-mesh and inflation layers. Face size is defined at the inlet and goes through the whole domain. Edge-sizing was used to give better mesh quality regarding orthogonal quality and aspect ratio, but without luck. See Figure 3.1. for the sweep-mesh from ANSYS Meshing.
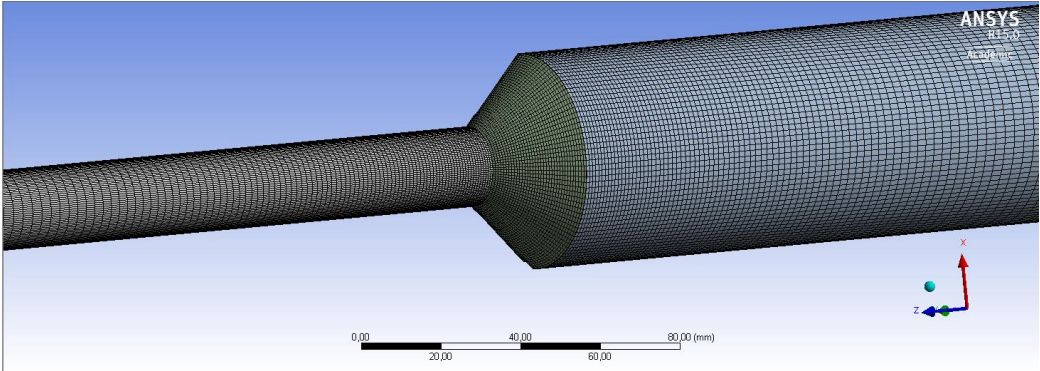
Hex mesh from ANSYS Meshing.

2. The tetra-mesh is much more unorganized, and more difficult to get control over the important quality aspects. With hex-cells in the inflation layers, the transition to the tetra-cells reduces the mesh quality. Also with its nodes-element ratio of 1:3, converged solutions is difficult to obtain. The mesh is shown in Figure 3.2.
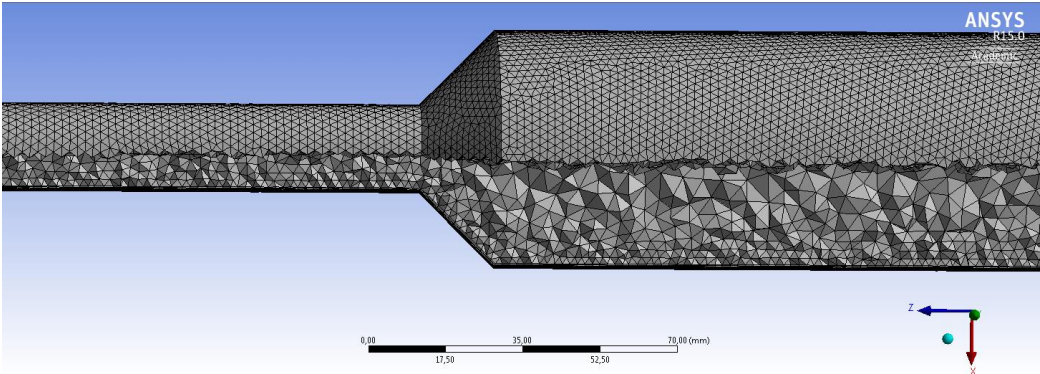
Tetra mesh from ANSYS Meshing.

61

Appendix B

DPM Simulation in Fluent – Input Summary

```
Fluent
Version: 3d, dp, pbns, sstkw (3d, double precision, pressure-based, SST
k-omega)
Release: 15.0.0
Title:

Models
------

   Model                      Settings
   -------------------------------------------------------------
   Space                      3D
   Time                       Steady
   Viscous                    SST k-omega turbulence model
   Heat Transfer              Disabled
   Solidification and Melting  Disabled
   Species                    Disabled
   Coupled Dispersed Phase    Enabled
   NOx Pollutants             Disabled
   SOx Pollutants             Disabled
   Soot                       Disabled
   Mercury Pollutants         Disabled

Material Properties
-------------------

   Material: sand (inert-particle)

      Property             Units    Method     Value(s)
      ---------------------------------------------------
      Density              kg/m3    constant   2600
      Cp (Specific Heat)   j/kg-k   constant   1680

   Material: air/co2 (fluid)

      Property                     Units    Method     Value(s)
      -----------------------------------------------------------------
      Density                      kg/m3    constant   24.136169
      Cp (Specific Heat)           j/kg-k   constant   1006.43
      Thermal Conductivity         w/m-k    constant   0.0242
      Viscosity                    kg/m-s   constant   1.5e-05
      Molecular Weight             kg/kgmol constant   28.966
      Reference Temperature        k        constant   309
      Thermal Expansion Coefficient 1/k     constant   0
      Speed of Sound               m/s      none       #f

   Material: aluminum (solid)

      Property             Units    Method     Value(s)
      ---------------------------------------------------
      Density              kg/m3    constant   2719
      Cp (Specific Heat)   j/kg-k   constant   871
```

62

```
         Thermal Conductivity   w/m-k    constant    202.4
Boundary Conditions
-------------------

    Zones

       name      id    type
       ----------------------------
       wall      1     wall
       inlet     2     velocity-inlet
       outlet    3     pressure-outlet

    Setup Conditions

       wall

          Condition                                          Value
          ----------------------------------------------------------------
-----------------------------------------------------------------------------
-----------------------------------------------------------------------------
-----------------------------------------------------------------------------
-----------------------------------------------------------------------------
-----------------------------------------------------------------------------
-----------------------------------------
          Enable shell conduction?                           no
          Wall Motion                                        0
          Shear Boundary Condition                           0
          Define wall motion relative to adjacent cell zone? yes
          Apply a rotational velocity to this wall?          no
          Velocity Magnitude (m/s)                           0
          X-Component of Wall Translation                    1
          Y-Component of Wall Translation                    0
          Z-Component of Wall Translation                    0
          Define wall velocity components?                   no
          X-Component of Wall Translation (m/s)              0
          Y-Component of Wall Translation (m/s)              0
          Z-Component of Wall Translation (m/s)              0
          Wall Roughness Height (m)                          0
          Wall Roughness Constant                            0.5
          Discrete Phase BC Type                             2
          Normal
0.80000001
          Tangent                                            1
          Discrete Phase BC Function                         none
          Impact Angle Function
((polynomial piecewise-linear angle (0 . 0) (0.052359872 . 0.38931575)
(0.10471974 . 0.62559682) (0.17453291 . 0.79820257) (0.23911008 .
0.87917018) (0.29670593 . 0.92019415) (0.40666166 . 0.9651503)
(0.52359873 . 0.99254328) (0.6352998 . 1.0018587) (0.69813162 .
0.99890703) (0.87266451 . 0.96232015) (1.0471975 . 0.89367861)
(1.2217304 . 0.79614067) (1.3962632 . 0.67655677) (1.5707961 .
0.56851071)))
          Diameter Function
((polynomial diameter 1.9999999e-09))
          Velocity Exponent Function
((polynomial normal-velocity 2.5999999))
          Rotation Speed (rad/s)                             0
```

```
     X-Position of Rotation-Axis Origin (m)              0
     Y-Position of Rotation-Axis Origin (m)              0
     Z-Position of Rotation-Axis Origin (m)              0
     X-Component of Rotation-Axis Direction              0
     Y-Component of Rotation-Axis Direction              0
     Z-Component of Rotation-Axis Direction              1
     X-component of shear stress (pascal)                0
     Y-component of shear stress (pascal)                0
     Z-component of shear stress (pascal)                0
     Fslip constant                                      0
     Eslip constant                                      0
     Specularity Coefficient                             0
     Enable Thermal Stabilization?                       no
     Scale Factor                                        0
     Stabilization Method                                1

  inlet

     Condition                                   Value
     -------------------------------------------------
     Velocity Specification Method               2
     Reference Frame                             0
     Velocity Magnitude (m/s)                    11.4
     Supersonic/Initial Gauge Pressure (pascal)  1410000
     Coordinate System                           0
     X-Velocity (m/s)                            0
     Y-Velocity (m/s)                            0
     Z-Velocity (m/s)                            0
     X-Component of Flow Direction               1
     Y-Component of Flow Direction               0
     Z-Component of Flow Direction               0
     X-Component of Axis Direction               1
     Y-Component of Axis Direction               0
     Z-Component of Axis Direction               0
     X-Coordinate of Axis Origin (m)             0
     Y-Coordinate of Axis Origin (m)             0
     Z-Coordinate of Axis Origin (m)             0
     Angular velocity (rad/s)                    0
     Turbulent Specification Method              3
     Turbulent Kinetic Energy (m2/s2)            1
     Specific Dissipation Rate (1/s)             1
     Turbulent Intensity (%)                     5
     Turbulent Length Scale (m)                  1
     Hydraulic Diameter (m)                      0.054
     Turbulent Viscosity Ratio                   10
     Discrete Phase BC Type                      4
     Discrete Phase BC Function                  none
     is zone used in mixing-plane model?         no

  outlet

     Condition                                   Value
     ------------------------------------------------------
     Gauge Pressure (pascal)                          0
     Backflow Direction Specification Method          1
     Coordinate System                                0
     X-Component of Flow Direction                    1
     Y-Component of Flow Direction                    0
```

```
                  Z-Component of Flow Direction              0
                  X-Component of Axis Direction              1
                  Y-Component of Axis Direction              0
                  Z-Component of Axis Direction              0
                  X-Coordinate of Axis Origin (m)            0
                  Y-Coordinate of Axis Origin (m)            0
                  Z-Coordinate of Axis Origin (m)            0
                  Turbulent Specification Method             3
                  Backflow Turbulent Kinetic Energy (m2/s2)  1
                  Backflow Specific Dissipation Rate (1/s)   1
                  Backflow Turbulent Intensity (%)           2.9999999
                  Backflow Turbulent Length Scale (m)        1
                  Backflow Hydraulic Diameter (m)            0.02
                  Backflow Turbulent Viscosity Ratio         10
                  Discrete Phase BC Type                     4
                  Discrete Phase BC Function                 none
                  is zone used in mixing-plane model?        no
                  Radial Equilibrium Pressure Distribution   no
                  Average Pressure Specification?            no
                                                             0
                  Specify targeted mass flow rate            no
                  Targeted mass flow (kg/s)                  1
                  Upper Limit of Absolute Pressure Value (pascal)  5000000
                  Lower Limit of Absolute Pressure Value (pascal)  1

   Solver Settings
   ---------------

      Equations

         Equation      Solved
         ------------------
         Flow          yes
         Turbulence    yes

      Numerics

         Numeric                       Enabled
         ---------------------------------------
         Absolute Velocity Formulation   yes

      Relaxation

         Variable                   Relaxation Factor
         ---------------------------------------------
         Pressure                   0.3
         Density                    1
         Body Forces                1
         Momentum                   0.7
         Turbulent Kinetic Energy   0.8
         Specific Dissipation Rate  0.8
         Turbulent Viscosity        1
         Discrete Phase Sources     0.5

      Linear Solver

                                  Solver    Termination   Residual
   Reduction
```

```
    Variable                    Type        Criterion   Tolerance
    -----------------------------------------------------------------
------
    Pressure                    V-Cycle     0.1
    X-Momentum                  Flexible    0.1         0.7
    Y-Momentum                  Flexible    0.1         0.7
    Z-Momentum                  Flexible    0.1         0.7
    Turbulent Kinetic Energy    Flexible    0.1         0.7
    Specific Dissipation Rate   Flexible    0.1         0.7

  Pressure-Velocity Coupling

    Parameter    Value
    -----------------
    Type         SIMPLE

  Discretization Scheme

    Variable                    Scheme
    ------------------------------------------------
    Pressure                    Second Order
    Momentum                    Second Order Upwind
    Turbulent Kinetic Energy    First Order Upwind
    Specific Dissipation Rate   First Order Upwind

  Solution Limits

    Quantity                    Limit
    ----------------------------------------
    Minimum Absolute Pressure   1
    Maximum Absolute Pressure   5e+10
    Minimum Temperature         1
    Maximum Temperature         5000
    Minimum Turb. Kinetic Energy  1e-14
    Minimum Spec. Dissipation Rate  1e-20
    Maximum Turb. Viscosity Ratio   100000
```

66

Appendix C

DDPM Simulation in Fluent with DNV – Input Summary

```
Fluent
Version: 3d, dp, pbns, eulerian, rke (3d, double precision, pressure-
based, Eulerian, realizable k-epsilon)
Release: 15.0.0
Title:

Models
------

    Model                         Settings
    ----------------------------------------------------------------
    Space                         3D
    Time                          Steady
    Viscous                       Realizable k-epsilon turbulence model
    Wall Treatment                Standard Wall Functions
    Multiphase k-epsilon Models   Mixture k-epsilon
    Heat Transfer                 Disabled
    Solidification and Melting    Disabled
    Species                       Disabled
    Coupled Dispersed Phase       Enabled
    NOx Pollutants                Disabled
    SOx Pollutants                Disabled
    Soot                          Disabled
    Mercury Pollutants            Disabled

Material Properties
-------------------

    Material: sand (inert-particle)

        Property              Units     Method     Value(s)
        ---------------------------------------------------
        Density               kg/m3     constant   2600
        Cp (Specific Heat)    j/kg-k    constant   1680

    Material: air/co2 (fluid)

        Property                      Units     Method     Value(s)
        ---------------------------------------------------------------
        Density                       kg/m3     constant   24.136169
        Cp (Specific Heat)            j/kg-k    constant   1006.43
        Thermal Conductivity          w/m-k     constant   0.0242
        Viscosity                     kg/m-s    constant   1.5e-05
        Molecular Weight              kg/kgmol  constant   28.966
        Reference Temperature         k         constant   309
        Thermal Expansion Coefficient 1/k       constant   0
        Speed of Sound                m/s       none       #f

    Material: aluminum (solid)

        Property                      Units     Method     Value(s)
        ---------------------------------------------------------------
```

```
        Density                 kg/m3    constant   2719
        Cp (Specific Heat)      j/kg-k   constant   871
        Thermal Conductivity    w/m-k    constant   202.4

Boundary Conditions
-------------------

    Zones

        name    id   type
        ---------------------------
        wall    1    wall
        inlet   2    velocity-inlet
        outlet  3    pressure-outlet

    Setup Conditions

        wall

        Condition                                           Value
        ----------------------------------------------------------
------------------------------------------------------------------------
------------------------------------------------------------------------
------------------------------------------------------------------------
------------------------------------------------------------------------
------------------------------------------------------------------------
------------------------------------------
        Enable shell conduction?                            no
        Wall Motion                                         0
        Shear Boundary Condition                            0
        Define wall motion relative to adjacent cell zone?  yes
        Apply a rotational velocity to this wall?           no
        Velocity Magnitude (m/s)                            0
        X-Component of Wall Translation                     1
        Y-Component of Wall Translation                     0
        Z-Component of Wall Translation                     0
        Define wall velocity components?                    no
        X-Component of Wall Translation (m/s)               0
        Y-Component of Wall Translation (m/s)               0
        Z-Component of Wall Translation (m/s)               0
        Wall Roughness Height (m)                           0
        Wall Roughness Constant                             0.5
        Discrete Phase BC Type                              2
        Normal
0.80000001
        Tangent                                             1
        Discrete Phase BC Function                          none
        Impact Angle Function
((polynomial piecewise-linear angle (0 . 0) (0.052359872 . 0.38931575)
(0.10471974 . 0.62559682) (0.17453291 . 0.79820257) (0.23911008 .
0.87917018) (0.29670593 . 0.92019415) (0.40666166 . 0.9651503)
(0.52359873 . 0.99254328) (0.6352998 . 1.0018587) (0.69813162 .
0.99890703) (0.87266451 . 0.96232015) (1.0471975 . 0.89367861)
(1.2217304 . 0.79614067) (1.3962632 . 0.67655677) (1.5707961 .
0.56851071)))
        Diameter Function
((polynomial diameter 1.9999999e-09))
```

```
            Velocity Exponent Function
((polynomial normal-velocity 2.5999999))
            Rotation Speed (rad/s)                          0
            X-Position of Rotation-Axis Origin (m)          0
            Y-Position of Rotation-Axis Origin (m)          0
            Z-Position of Rotation-Axis Origin (m)          0
            X-Component of Rotation-Axis Direction          0
            Y-Component of Rotation-Axis Direction          0
            Z-Component of Rotation-Axis Direction          1
            X-component of shear stress (pascal)            0
            Y-component of shear stress (pascal)            0
            Z-component of shear stress (pascal)            0
            Fslip constant                                  0
            Eslip constant                                  0
            Specularity Coefficient                         0
            Enable Thermal Stabilization?                   no
            Scale Factor                                    0
            Stabilization Method                            1

      inlet

            Condition                                 Value
            -------------------------------------------------
            Supersonic/Initial Gauge Pressure (pascal)  0
            Turbulent Specification Method              3
            Turbulent Kinetic Energy (m2/s2)            1
            Turbulent Dissipation Rate (m2/s3)          1
            Turbulent Intensity (%)                     5
            Turbulent Length Scale (m)                  1
            Hydraulic Diameter (m)                      0.054
            Turbulent Viscosity Ratio                   10
            Discrete Phase BC Type                      4
            Discrete Phase BC Function                  none
            is zone used in mixing-plane model?         no

      outlet

            Condition                                 Value
            -----------------------------------------------------
            Gauge Pressure (pascal)                     0
            Backflow Direction Specification Method     1
            Turbulent Specification Method              3
            Backflow Turbulent Kinetic Energy (m2/s2)   1
            Backflow Turbulent Dissipation Rate (m2/s3) 1
            Backflow Turbulent Intensity (%)            2.9999999
            Backflow Turbulent Length Scale (m)         1
            Backflow Hydraulic Diameter (m)             0.02
            Backflow Turbulent Viscosity Ratio          10
            Discrete Phase BC Type                      4
            Discrete Phase BC Function                  none
            is zone used in mixing-plane model?         no
            Radial Equilibrium Pressure Distribution    no

Solver Settings
---------------

   Equations
```

```
      Equation          Solved
      -----------------------
      Flow              yes
      Volume Fraction   yes
      Turbulence        yes

   Numerics

      Numeric                       Enabled
      ---------------------------------------
      Absolute Velocity Formulation   yes

   Relaxation

      Variable                      Relaxation Factor
      -------------------------------------------
      Pressure                      0.3
      Density                       1
      Body Forces                   1
      Momentum                      0.7
      Volume Fraction               0.5
      Granular Temperature          0.2
      Turbulent Kinetic Energy      0.8
      Turbulent Dissipation Rate    0.8
      Turbulent Viscosity           1
      Discrete Phase Sources        0.5

   Linear Solver

                                    Solver     Termination   Residual
Reduction
      Variable                      Type       Criterion     Tolerance
      ------------------------------------------------------------------
-------
      Pressure                      V-Cycle    0.1
      X-Momentum                    Flexible   0.1           0.7
      Y-Momentum                    Flexible   0.1           0.7
      Z-Momentum                    Flexible   0.1           0.7
      Volume Fraction               Flexible   0.1           0.7
      Turbulent Kinetic Energy      Flexible   0.1           0.7
      Turbulent Dissipation Rate    Flexible   0.1           0.7

   Pressure-Velocity Coupling

      Parameter    Value
      --------------------------------
      Type         Phase Coupled SIMPLE

   Discretization Scheme

      Variable                      Scheme
      ------------------------------------------------
      Momentum                      First Order Upwind
      Volume Fraction               First Order Upwind
      Turbulent Kinetic Energy      First Order Upwind
      Turbulent Dissipation Rate    First Order Upwind

   Solution Limits
```

```
Quantity                      Limit
--------------------------------------
Minimum Absolute Pressure     1
Maximum Absolute Pressure     5e+10
Minimum Temperature           1
Maximum Temperature           5000
Minimum Turb. Kinetic Energy  1e-14
Minimum Turb. Dissipation Rate 1e-20
Maximum Turb. Viscosity Ratio 100000
```

```
Minimum Turb. Kinetic Energy
```

Appendix D

DDPM Simulation in Fluent with Abrasive – Boundary Conditions

```
Setup Conditions

   wall

      Condition                                         Value
      ----------------------------------------------------------------
----------------------------------------------------------
      Enable shell conduction?                          no
      Wall Motion                                       0
      Shear Boundary Condition                          0
      Define wall motion relative to adjacent cell zone?  yes
      Apply a rotational velocity to this wall?         no
      Velocity Magnitude (m/s)                          0
      X-Component of Wall Translation                   1
      Y-Component of Wall Translation                   0
      Z-Component of Wall Translation                   0
      Define wall velocity components?                  no
      X-Component of Wall Translation (m/s)             0
      Y-Component of Wall Translation (m/s)             0
      Z-Component of Wall Translation (m/s)             0
      Wall Roughness Height (m)                         0
      Wall Roughness Constant                           0.5
      Discrete Phase BC Type                            2
      Normal
0.80000001
      Tangent                                           1
      Discrete Phase BC Function                        none
      Impact Angle Function
((polynomial piecewise-linear angle (0 . 1) (1.5707961 . 1)))
      Diameter Function
((polynomial diameter 1.9e-08))
      Velocity Exponent Function
((polynomial normal-velocity 1.41))
      Rotation Speed (rad/s)                            0
      X-Position of Rotation-Axis Origin (m)            0
      Y-Position of Rotation-Axis Origin (m)            0
      Z-Position of Rotation-Axis Origin (m)            0
      X-Component of Rotation-Axis Direction            0
      Y-Component of Rotation-Axis Direction            0
      Z-Component of Rotation-Axis Direction            1
      X-component of shear stress (pascal)              0
      Y-component of shear stress (pascal)              0
      Z-component of shear stress (pascal)              0
      Fslip constant                                    0
      Eslip constant                                    0
      Specularity Coefficient                           0
      Enable Thermal Stabilization?                     no
      Scale Factor                                      0
      Stabilization Method                              1
```

inlet

```
Condition                                    Value
-------------------------------------------------------
Supersonic/Initial Gauge Pressure (pascal)   0
Turbulent Specification Method               3
Turbulent Kinetic Energy (m2/s2)             1
Turbulent Dissipation Rate (m2/s3)           1
Turbulent Intensity (%)                      2.9999999
Turbulent Length Scale (m)                   1
Hydraulic Diameter (m)                       0.054
Turbulent Viscosity Ratio                    10
Discrete Phase BC Type                       4
Discrete Phase BC Function                   none
is zone used in mixing-plane model?          no
```

outlet

```
Condition                                    Value
-------------------------------------------------------
Gauge Pressure (pascal)                      0
Backflow Direction Specification Method      1
Turbulent Specification Method               3
Backflow Turbulent Kinetic Energy (m2/s2)    1
Backflow Turbulent Dissipation Rate (m2/s3)  1
Backflow Turbulent Intensity (%)             2.9999999
Backflow Turbulent Length Scale (m)          1
Backflow Hydraulic Diameter (m)              0.02
Backflow Turbulent Viscosity Ratio           10
Discrete Phase BC Type                       4
Discrete Phase BC Function                   none
is zone used in mixing-plane model?          no
Radial Equilibrium Pressure Distribution     no
```